

Journal Pre-proof

Discovery of novel 1,2,3-triazole oseltamivir derivatives as potent influenza neuraminidase inhibitors targeting the 430-cavity

Han Ju, Siyu Xiu, Xiao Ding, Min Shang, RuiFang Jia, Bing Huang, Peng Zhan, Xinyong Liu



PII: S0223-5234(19)31092-X

DOI: <https://doi.org/10.1016/j.ejmech.2019.111940>

Reference: EJMECH 111940

To appear in: *European Journal of Medicinal Chemistry*

Received Date: 16 September 2019

Revised Date: 19 November 2019

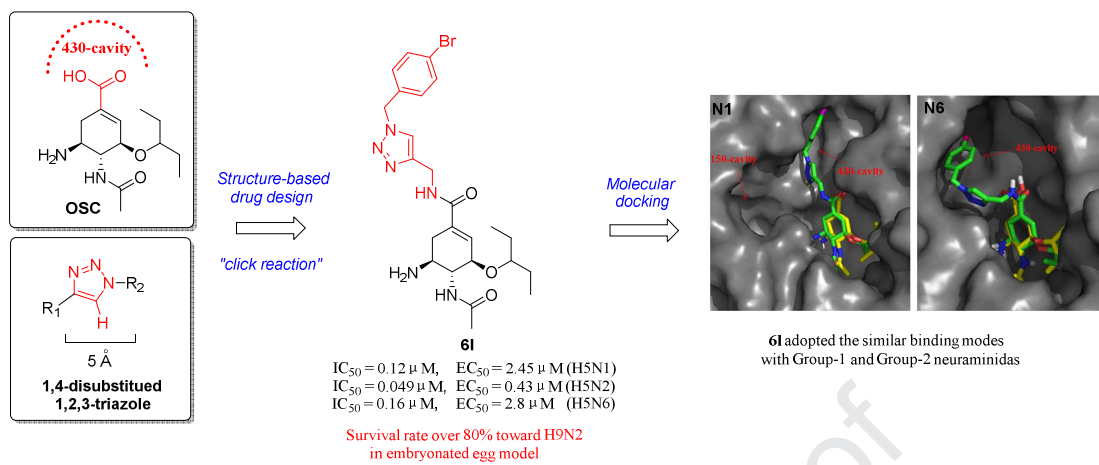
Accepted Date: 2 December 2019

Please cite this article as: H. Ju, S. Xiu, X. Ding, M. Shang, R. Jia, B. Huang, P. Zhan, X. Liu, Discovery of novel 1,2,3-triazole oseltamivir derivatives as potent influenza neuraminidase inhibitors targeting the 430-cavity, *European Journal of Medicinal Chemistry* (2020), doi: <https://doi.org/10.1016/j.ejmech.2019.111940>.

This is a PDF file of an article that has undergone enhancements after acceptance, such as the addition of a cover page and metadata, and formatting for readability, but it is not yet the definitive version of record. This version will undergo additional copyediting, typesetting and review before it is published in its final form, but we are providing this version to give early visibility of the article. Please note that, during the production process, errors may be discovered which could affect the content, and all legal disclaimers that apply to the journal pertain.

© 2019 Published by Elsevier Masson SAS.

Graphical abstract



Discovery of novel 1,2,3-triazole oseltamivir derivatives as potent influenza neuraminidase inhibitors targeting the 430-cavity

Han Ju^a, Siyu Xiu^a, Xiao Ding^a, Min Shang^b, RuiFang Jia^a, Bing Huang^{b,*}, Peng

Zhan^{a,*}, Xinyong Liu^{a,*}

^a*Department of Medicinal Chemistry, Key Laboratory of Chemical Biology (Ministry of Education), School of Pharmaceutical Sciences, Shandong University, 44 West Culture Road, 250012 Jinan, Shandong, PR China*

^b*Institute of Poultry Science, Shandong Academy of Agricultural Sciences, 1, Jiaoxiao Road, 250023 Jinan, Shandong, PR China*

Abstract

A novel series of 1,2,3-triazole oseltamivir derivatives, which could simultaneously occupy the classical NA catalytic site and the newly reported 430-cavity, were designed, synthesized, and evaluated for their anti-influenza activities. The results demonstrated that four compounds (**6g**, **6l**, **6y** and **8c**) showed robust anti-influenza potencies against H5N1, H5N2 and H5N6 strains in both enzymatic assay and cellular assay. Especially, **6l** was proved to possess the most potent and broad-spectrum anti-influenza activity, with IC₅₀ values of 0.12 μM, 0.049 μM and 0.16 μM and EC₅₀ values of 2.45 μM, 0.43 μM and 2.8 μM against H5N1, H5N2 and H5N6 strains, respectively, which were slightly weaker than oseltamivir carboxylate. In addition, in the embryonated egg model, **6l** achieved the similar protective effect against H9N2 strain with oseltamivir carboxylate in the tested concentrations. Preliminary structure-activity relationships (SARs), molecular modeling, and calculated

physicochemical properties of selected compounds were also discussed.

Keywords: Influenza virus, Neuraminidase inhibitors, 430-cavity, Oseltamivir derivatives, Broad-spectrum anti-influenza activity.

1. Introduction

Influenza A and B viruses (FluA and FluB) are respiratory pathogens that cause an infectious disease annually associated with 290,000 to 650,000 deaths and 3 to 5 million hospitalizations worldwide, especially among high risk people such as elder and patient with immunocompromised or cardiovascular diseases [1]. FluA can also confer recurring pandemics, which caused devastating effects on global population in terms of prevalence and morbidity in the past (e.g., 1918 H1N1, 1968 H3N2 and 2009 H1N1pdm09) [2]. Additionally, H5N1 and H7N9 avian FluA have crossed the species barrier and lead to thousands of documented zoonotic outbreaks in humans with high mortality (e.g., H5N1: 63%, H7N9: 40%) in recent years [3-5]. Although there is no established evidence of efficient human-to-human transmission, their pandemic potential is clear and poses a serious and constant threat to global public health.

Vaccination is the main method to prevent influenza infections, but the continuous evolution of influenza virus to avoid host detection system by changing its antigenicity on hemagglutinin (HA), render existing vaccines useless. And a 6-month time gap between WHO recommendation and the actual application of vaccines dramatically decrease its effectiveness against the strains in influenza circulation [6].

Therefore, using antiviral drugs to block the functional proteins of virus is the most efficient method for managing influenza infections.

Neuraminidase (NA), a surface glycoprotein that facilitates the releasing and propagating of newly formed virions, is a promising target for anti-influenza drugs design [7]. Moreover, attributing to their low toxicity, high selectivity and potent anti-influenza potency, neuraminidase inhibitors (NAIs: oseltamivir, zanamivir, peramivir and laninamivir octanoate, **Fig. 1**) function as the only class of antiviral available clinically [8]. However, the rapid emergence and spread of drug-resistant influenza strains seriously compromised their clinical application. Among them, H274Y is the most prevalent resistance-associated mutations towards oseltamivir which was widely used as preferred drug in clinic since its approval in 1999 [9, 10]. Additionally, E119G and R292K are also observed resistance mutations in the treatment of zanamivir and peramivir, respectively [11, 12], and one isolated I117T mutation of NA shows cross-resistance to both oseltamivir and zanamivir [13]. Consequently, there is a clear need to develop improved NAIs for effective influenza therapy.

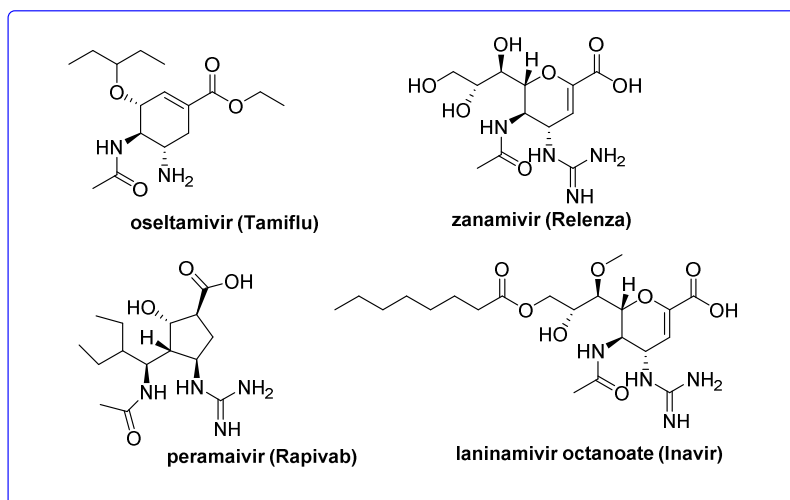


Fig. 1. Structures of approved NA inhibitors

On the basis of the X-ray crystallographic studies, newly reported 150-cavity (formed by 150-loop) and 430-cavity (formed by 430-loop) which directly connect with the classical NA catalytic site are revealed as two broad regions for accommodating further NAIs design [14-19]. In fact, in recent years, the breakthrough has been made in our lab by modifying the C5-NH₂ of oseltamivir for probing 150-cavity, and several obtained compounds (**Fig. S1**) have displayed dozens of times greater anti-influenza activity than oseltamivir carboxylate (OSC, the active form of oseltamivir), including against oseltamivir-resistance strains [20-22]. Our previous work supported the idea well that addition of substituents to the oseltamivir core could result in strong interactions with the 150-cavity and increase the affinity with NA. However, most of the oseltamivir derivatives targeting 150-cavity cannot exert a broad-spectrum anti-influenza activity, because 150-cavity only exists in group-1 NAs (containing N1, N4, N5, and N8,). This is influenced by the conformation of 150-loop, that is, the 150-cavity will not be formed when 150-loop is at a close state. In contrast, 430-loop is always in a stably opened conformation, resulting in 430-cavity widely existing in all group-1 and group-2 NAs (containing N2, N3, N6, N7, and N9, **Fig. 2**). Therefore, in theory, modifications of NAIs targeting 430-cavity have better prospects than targeting 150-cavity.

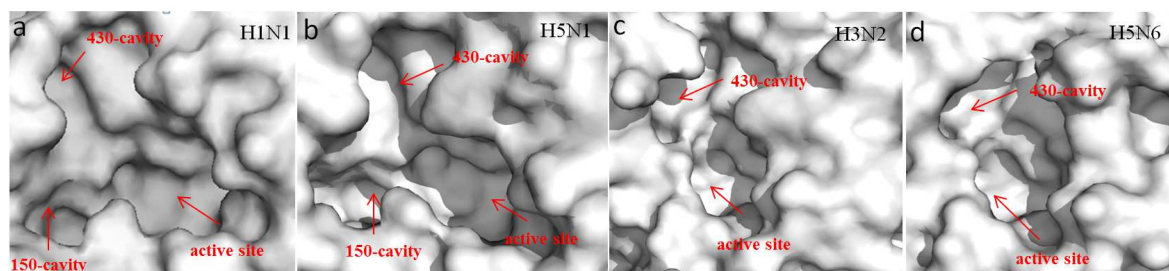


Fig. 2. Comparison of the crystal structures of the Group-1 NA (a, b) and Group-2 NA (c, d) subtypes. Structures of N1 (H1N1, PDB code: 3BEQ; H5N1, PDB code: 2HU0), N2 (H3N2, PDB code: 4GZP) and N6 (H5N6, PDB code: 5HUM) are in surface representation. The catalytic pocket, 430-cavity and opened 150-cavity are labeled in red arrows.

Close examination of the crystal structure of OSC bound to the NA indicated that the C-1 carboxyl group of OSC was well exposed towards the 430-cavity. Given the attractiveness of the 430-cavity as an additional binding pocket, and the wealth of co-crystal structures available, we chose C-1 position of OSC to focus our optimization efforts upon. Specifically, the Cu(I)-catalyzed azide and alkyne 1,3-dipolar cycloaddition (CuAAC), commonly known as the "click reaction", facilitates the formation of 1,4-disubstituted 1,2,3-triazole ring which is usually used as linker in drug optimization [23,24]. Moreover, owing to the unique properties of 1,2,3-triazole ring, such as rigidity and stability *in vivo*, hydrogen bonding capability and suitable length (about 5Å), this unit is considered as decisive factor for improving the biological activities of the compounds in medicinal chemistry [25]. Therefore, we decided to introduce 1,2,3-triazole unit as a linker to connect various substituents with suitable shape, size, and/or hydrophobicity at the C-1 position of OSC. And we hoped that the modified C-1 side chain could extend into the 430-cavity and engender potentially additional interactions with the surrounding residue in the

cavity to enhance the affinity, the broad-spectrum and anti-resistance properties of the compounds (**Fig. 3**). Eventually, 33 novel oseltamivir analogues were designed, synthesized and evaluated for their biological activities.

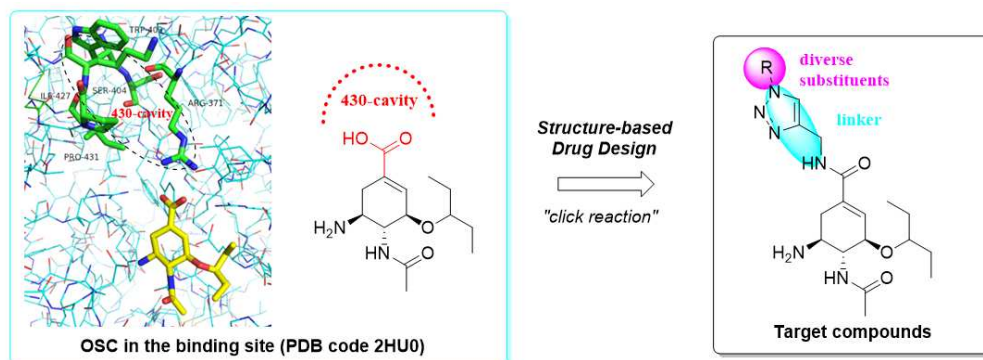
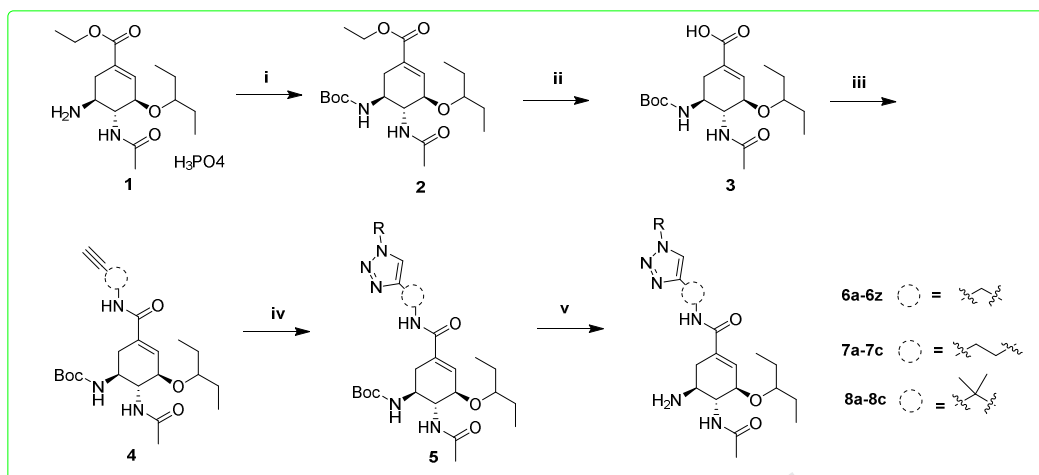


Fig. 3 The design of novel C-1 modified oseltamivir derivatives targeting 430-cavity.

2. Results and discussion

2.1. Chemistry

The general synthetic steps adopted to obtain the target compounds were straightforwardly outlined in **Scheme 1**. These target compounds were synthesized from the commercially available starting material oseltamivir phosphate (**1**). Firstly, **1** reacted with Boc anhydride in methanol and Et_3N to produce **2**, which was hydrolyzed by NaOH to give the intermediate **3** [26]. In the presence of HATU, intermediate **3** reacted with different ynamines to afford **4**. And then, **5** was generated by CuAAC “click chemistry” reaction between the substituted azides and intermediate **4**. Finally, intermediate **5** was directly deprotected with 12 M HCl in methanol to afford the target compounds **6a-6z**, **7a-7c** and **8a-8c**. The newly synthesized compounds were characterized by HRMS and NMR spectra.



Scheme 1. Reagents and conditions: (i) (Boc)₂O, Et₃N, methanol, RT; (ii) 4 M NaOH, RT; (iii) corresponding ynamines, HATU, Et₃N, CH₂Cl₂, RT; (iv) RN₃, CuSO₄, L-ascorbic acid sodium salt, THF, H₂O, RT; (v) 12 M HCl, methanol, RT.

2.2. Biological activity

2.2.1. *In vitro* inhibitory activities on NAs

All the newly designed oseltamivir derivatives were screened for NA inhibitory activities using a fluorescence-based assay with MUNANA as the substrate [20-22, 26]. For broad-spectrum NA inhibition screening, we chose N1 (H5N1) from group-1, N2 (H5N2) and N6 (H5N6) from group-2 as representatives for testing. OSC and zanamivir (ZA) were run in parallel as control drugs. The measured inhibition potencies of the synthesized compounds are summarized in **Table 1**. It was clear that OSC showed great inhibitory potency toward wild-type NAs with IC₅₀ values of 20 nM, 7 nM and 18 nM against H5N1, H5N2 and H5N6, respectively. Zanamivir, another positive control drug, displayed comparable activity with oseltamivir against H5N1 (IC₅₀ = 12 nM), H5N2 (IC₅₀ = 21 nM) and H5N6 NAs (IC₅₀ = 22 nM), which

was consistent with reported data [21, 22].

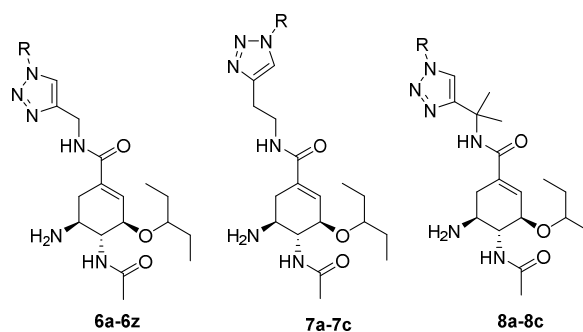
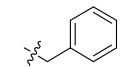
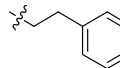
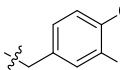
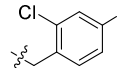
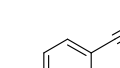
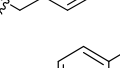
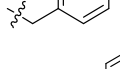
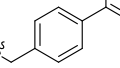
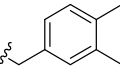
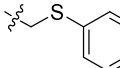
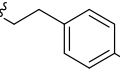
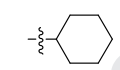
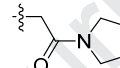
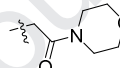
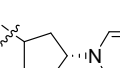
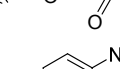
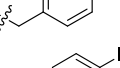
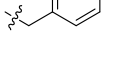
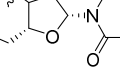
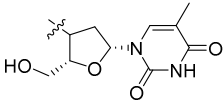


Table 1. Structures and *in vitro* inhibitory effects of test compounds against influenza NAs.

Compds	R	IC ₅₀ (μM) ^a		
		H5N1 ^b	H5N2 ^c	H5N6 ^d
6a		>10	0.86±0.069	>10
6b		0.58±0.033	1.19±0.06	2.85±0.34
6c		0.98±0.035	0.86±0.07	1.17±0.09
6d		1.59±0.15	>10	1.67±0.26
6e		1.08±0.17	2.2±0.11	2.0±0.18
6f		2±0.18	2.11±0.16	3.2±0.15
6g		0.48±0.08	0.14±0.03	0.13±0.01
6h		7.15±1.05	0.92±0.35	2.56±0.03
6i		3.17±0.29	1.27±0.06	3.28±0.12
6j		0.64±0.02	2.29±0.38	>10
6k		4.1±0.33	2.32±0.11	4.3±0.9
6l		0.12±0.002	0.049±0.007	0.16±0.007

6m		2.45±0.5	0.66±0.008	1±0.19
6n		4.05±0.07	0.36±0.024	0.57±0.02
6o		1.53±0.11	0.82±0.1	2.8±0.7
6p		2.14±0.17	2.42±0.27	2.4±0.08
6q		2.72±0.14	1.96±0.15	2.86±0.03
6r		3.86±0.14	2.18±0.19	5.5±0.24
6s		1.41±0.15	1.13±0.06	2.2±0.43
6t		3.12±0.26	2.78±0.17	3.1±0.12
6u		3.17±0.03	3.44±0.16	4.59±0.2
6v		3.96±0.22	4.54±0.1	6.34±0.66
6w		1.58±0.07	1.6±0.16	2.01±0.1
6x		1.89±0.06	0.78±0.007	1.4±0.16
6y		0.53±0.05	0.38±0.04	0.79±0.01
6z		0.44±0.07	0.69±0.082	0.29±0.05
7a		4.63±0.33	3.48±0.22	7.6±0.55
7b		>10	8.86±1.12	>10
7c		7.69±0.25	5.66±0.27	>10
8a		7.8±0.5	5.23±0.4	>10
8b		>10	4.05±1.2	>10

8c		0.46±0.06	0.49±0.03	0.58±0.13
OSC	-----	0.020±0.002	0.007±0.001	0.018±0.001
ZA	-----	0.012±0.001	0.021±0.00008	0.022±0.001

^aConcentration required to reduce NA activity to 50% of control NA activity (IC₅₀). Data are shown as mean ± SD of three experiments.

^bA/Goose/Guangdong/SH7/2013 (H5N1).

^cA/Chicken/Hebei/LZF/2014 (H5N2).

^dA/Duck/Guangdong/674/2014 (H5N6).

As shown in **Table 1**, the biological results clearly showed that most of the newly synthesized compounds exhibited anti-NAs activities from micromolar to sub-micromolar ranges. Impressively, several of the designed compounds (**6c**, **6g**, **6l**, **6n**, **6y** and **6z**) displayed robust inhibitory potencies against all three NAs, and in particular, **6l** achieved the most potent activity with the IC₅₀ values of 0.12 μM, 0.049 μM and 0.16 μM against H5N1, H5N2 and H5N6 NAs, respectively, being slightly weaker than that of OSC and ZA. On the basis of the above results, the preliminary SARs could be concluded in terms of different terminal substitution groups and the length of the side chain.

For the former, an aromatic ring might be sterically and electronically complementary to the 430-cavity, and compounds **6a-6v** were designed with various substituted benzene rings. Detailed comparison of the data of compounds **6a-6l**, we found that variation of the position of the identical substituent in the benzene (from the *ortho*-position to the *para*-position) resulted in different inhibitory activities. As for fluorine atom substituent, compounds **6d-6f** had similar inhibition against three NAs with the IC₅₀ values ranging from 1 μM to 3 μM no matter which position the fluorine atom was introduced. However, in the case of bearing a nitro group or a

chlorine atom, the order of potencies against NAs was **6b** (3-NO₂) \approx **6c** (4-NO₂) > **6a** (2-NO₂) and **6g** (2-Cl) > **6i** (4-Cl) > **6h** (3-Cl). Surprisingly, compound **6l** with a bromine atom at *para*-position of benzene ring showed the greatest activities for all NAs in this series, but the activities decreased sharply when moved the bromine atom to *ortho*- (**6j**) or *meta*-position (**6k**). Likewise, replacing 4-Br of **6l** with 4-nitrile (**6q**), 4-methyl (**6r**), 4-phenyl (**6s**) or non-substituent (**6m**) also resulted in activities decline against all the NAs. Next, comparison of activities of **6g** and **6l** with **6o** (IC₅₀ = 0.82-2.8 μ M) and **6p** (IC₅₀ = 2.14-2.4 μ M) indicated that mono-substituted derivatives of halogen atom were preferred than di-substituted ones distinctly. In addition, pairwise comparison of the activities (compounds **6m** vs **6n** and **6l** vs **6v**) suggested that the length of side chain at the end of 1,2,3-triazole could not govern the anti-NA activities proportionally or inversely.

To extend the SAR information, we designed compounds **6w-6z** by replacing the benzene ring with heteroatomic naphthenes. Among them, compounds **6y** and **6z** bearing a morpholine ring and a Zidovudine motif, respectively, were more advantageous for inhibitory activities against all three NAs than benzene-contained derivatives except for compounds **6h** and **6l**. Thus, it appeared that a moderately flexible group at the end of side chain might more sensitive to NA.

Inspired by the result of **6a-6z**, we further designed two subseries of compounds **7a-7c** and **8a-8c** with the C-1 modification at the position between the amide bond and 1,2,3-triazole linker. However, with a negative impact on the anti-NA activities, most of the compounds lost the potency (IC₅₀>10 μ M) against H5N1 and H5N6 NAs,

and as for H5N2 NA, their inhibition were also very weak. But encouragingly, compound **8c** exhibited considerably enhanced anti-NA activity with the IC_{50} of 0.46 μ M, 0.49 μ M and 0.58 μ M against H5N1, H5N2 and H5N6 NAs, respectively.

Next, we selected compounds **6c**, **6g**, **6l**, **6n**, **6y**, **6z** and **8c** as representatives to investigate their potencies against H5N1-H274Y NA, because the clinical strain with this NA mutant exhibits high-level resistance to oseltamivir, which is presently of a great concern. We used the same assay as above and the data was shown in **Table 2**. In agreement with previous reports [21, 22], this mutant conferred resistance to OSC with the potency ($IC_{50} = 3.38 \mu$ M) over 160-fold weaker than that of wild-type H5N1 NA, but its susceptibility to zanamivir ($IC_{50} = 0.013 \mu$ M) was not altered. Apart from **6g** and **6l**, all the tested compounds showed weak inhibitory activities ($IC_{50} > 100 \mu$ M) against H5N1-H274Y mutation. But notably, compound **6l** displayed robust activity against H5N1-H274Y, with IC_{50} values of 23.8 μ M, which was 7 times weaker relative to OSC. These results were in consistent with the inhibitory effects against wild-type H5N1 NA, but their potencies did not support the design strategy well that modification at C-1 side chain targeting 430-cavity could improve their anti-resistance profiles.

Table 2. NA (H5N1-H274Y) inhibitory activities of selected compounds ^a

Compds	IC_{50} (μ M)
	H5N1-H274Y
6c	>150
6g	79.2 \pm 1.9
6l	23.8 \pm 2.1

6n	>150
6y	106.1±5.1
6z	>150
8c	122.7±3.7
OSC	3.38±0.07
ZA	0.013±0.00035

^aData are shown as mean ± SD of three experiments.

2.2.2 Molecular modeling analysis

In order to obtain further insight into the binding of 1,2,3-triazole oseltamivir derivatives to the biologically relevant chemical space of NA, by means of software SYBYL-X 2.0, the most potent compound **6l** was subjected to further docking studies utilizing the structures of co-crystal of NA (PDB code: 2HU0 (Group-1, N1) and 5HUM (Group-2, N6)) [26,27]. The amino acid sequences of tested NAs are highly similar to that of PDBs (N1>90% and N6>99%, shown in supplementary material), and these inconsistent amino acid residues are far from NA catalytic center or the 430-cavity, which greatly increases the credibility of the docking analysis. Our docking results were visualized by PyMOL.

As shown in **Fig. 4a**, the docking simulations of **6l** with N1 revealed that the binding mode resembled its lead compound OSC in active center, and of particular note was that the elongated C-1 side chain was projected toward the 430-cavity. In **Fig. 4b**, compound **6l** developed four hydrogen bonds with Arg371, Tyr406 and Arg152 in active center, and the 1,2,3-triazole group also formed additional double hydrogen bonds with Arg118. Meanwhile, the 1,2,3-triazole linked 4-bromobenzyl group stretched into the 430-cavity and occupied a small hydrophobic pocket

consisted of Pro431, Lys432, Ser370 and the backbone of Arg371. These docking results showed that **6l** could simultaneously occupy the classical NA catalytic site and 430-cavity which was consistent with our original design intention and thereby displaying great NA inhibition.

As observed in the X-ray crystal structure of N6 bound to **6l** (**Fig. 4c**), this binding mode resembled OSC in parent scaffold and the 4-bromobenzyl group also extended into the 430-cavity as the fragment located. Similarly, compound **6l** maintained the typical hydrogen bonds with the same residues around active center and 430-cavity like that of N1, though their residue serial number were different in 2HU0 and 5HUM (**Fig. 4d**). Comparing the above two binding modes, we found that the modified C-1 amide bond developed four hydrogen bonds with residues Arg214, Arg293 and Tyr327 in N6, but only three hydrogen bonds were observed in the same region in N1. However, the 1,2,3- triazole group of compound **6l** could form one more hydrogen bond with Arg118 in N1 than in N6, which might compensate for affinity loss at the amide bond. Therefore, the similar binding modes adopted and the same number of hydrogen bonds formed in the binding pockets could provide a rational explanation of the equally broad-spectrum NA inhibitory activity for this molecule. On the other hand, compared with OSC, the hydrogen bonds with Arg292 and Tyr347 were not observed in the modes of **6l**, which might be the main reason for the reduced anti-NA activity of **6l** relative to OSC (**Fig. S2**). To sum up, the molecular modeling analysis explained the theoretical binding mode and the potent activity of compound **6l**, which was consistent with our design and would assist further structural optimization.

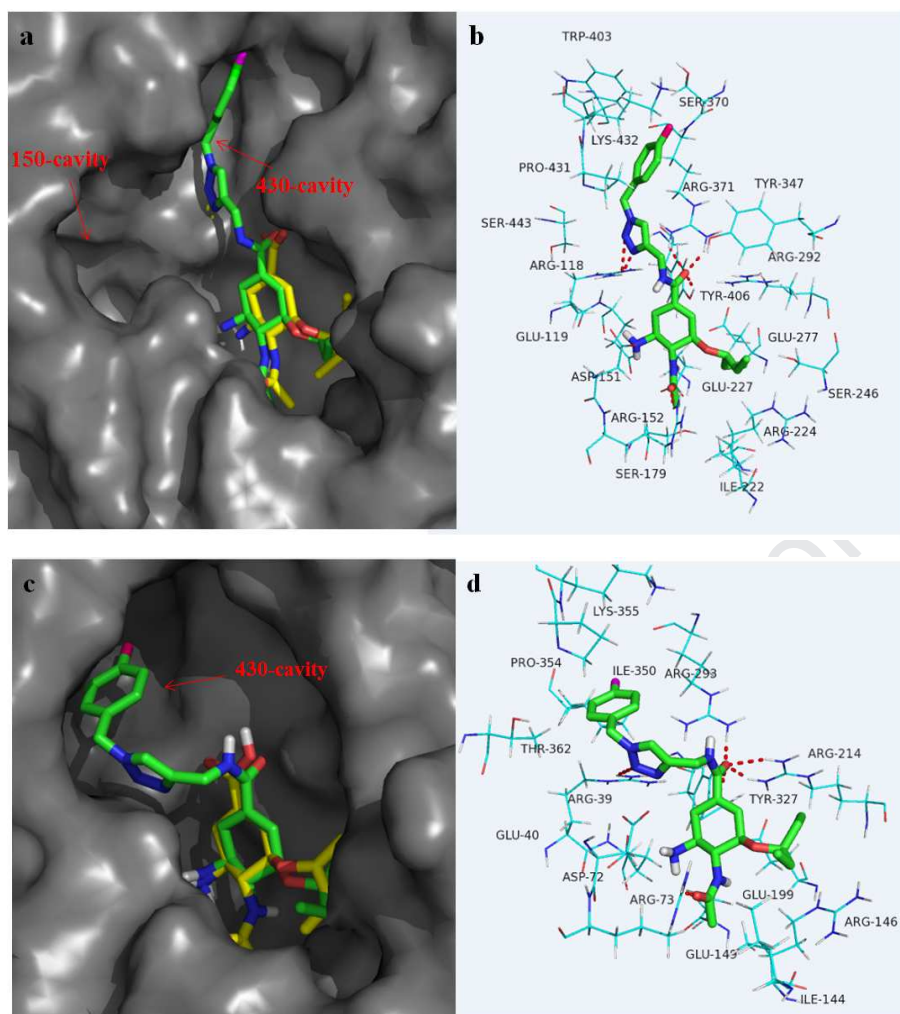


Fig.4. Predicted binding modes of compound **6I** (green) with Group-1 NA (H5N1, PDB code: 2HU0) and Group-2 NA (H5N6, PDB code: 5HUM). (a) Superposition of the binding modes of **6I** (green) and OSC (yellow) in H5N1 NA; (b) The key residues of H5N1 (azure) that form potential interactions with compound **6I**; (c) Superposition of the binding modes of **6I** (green) and OSC (yellow) in H5N6 NA; (d) The key residues of H5N6 (azure) that form potential interactions with compound **6I**. Hydrogen bonds between inhibitor and amino acid residues are indicated with dashed lines (red).

2.2.3 *In vitro* anti-influenza virus activity

To validate the efficacy of the synthesized compounds against influenza virus infection, we employed cell-based assay (chicken embryo fibroblasts, CEFs) that

addressed the cytopathic effect (CPE) of influenza virus infection using the same virus strains with anti-NA assay [21, 27-28]. We further chose **6g**, **6l**, **6y** and **8c** as representatives, and used oseltamivir carboxylate (OSC) as reference compound in parallel. The results were expressed as EC₅₀ and CC₅₀ summarized in **Table 3**. Notably, all the tested compounds exhibited no appreciable cytotoxicity at the highest tested concentrations (CC₅₀ > 1000 μM) in CEFs.

Table 3. *In vitro* anti-influenza virus activities in CEFs

Compds	EC ₅₀ (μM) ^a	EC ₅₀ (μM)	EC ₅₀ (μM)	CC ₅₀ (μM) ^b	SI ^g
	H5N1 ^c	H5N2 ^d	H5N6 ^e		(H5N1)
6g	3.32±0.07	0.47±0.06	8.6±4.2	>1000	>300
6l	2.45±0.2	0.43±0.04	2.8±0.5	>1000	>400
6y	3.1±0.2	1±0.15	3.78±0.2	>1000	>330
8c	6.28±0.8	0.53±0.02	>20	>1000	>160
OSC	0.22±0.01	0.18±0.02	0.43±0.12	>1000	>4500

^aEC₅₀: concentration required to achieve 50% protection against virus-induced cytopathic effect.

^bCC₅₀: concentration of 50% cellular toxicity.

^cA/Goose/Guangdong/SH7/2013 (H5N1).

^dA/Chicken/Hebei/LZF/2014 (H5N2).

^eA/Duck/Guangdong/674/2014 (H5N6)

^gSI: selectivity index, the ratio of CC₅₀/EC₅₀.

In the case of the H5N1 virus, **6l** displayed the greatest activity (EC₅₀ = 2.45 μM), which was about 11 folds weaker than OSC (EC₅₀ = 0.22 μM), and the values of other compounds were 15-30 times lower than positive control. Additionally, we obtained similar results against H5N6 virus, that **6l** also exerted the best activity (EC₅₀ = 2.8

μM) which however was 6 folds weaker than OSC ($\text{EC}_{50} = 0.43 \mu\text{M}$), and the potencies of other compounds were sharply reduced. These results were in line with the data in enzymatic assay and compound **6l** still displayed the best antiviral potency towards H5N1 and H5N6 strains.

Surprisingly, against H5N2 virus, compounds **6g**, **6l**, and **8c** shown great antiviral activities, with EC_{50} values of $0.43 \mu\text{M}$, $0.47 \mu\text{M}$ and $0.53 \mu\text{M}$, which was comparable to OSC ($\text{EC}_{50} = 0.18 \mu\text{M}$). And the weakest compound tested also exerted moderate antiviral activity (**6y**, $\text{EC}_{50} = 1 \mu\text{M}$). The results indicated that these 1,2,3-triazole derivatives were more sensitive to H5N2 virus than other two strains at least in cellular level.

Overall, the antiviral activities of oseltamivir derivatives **6g**, **6l**, **6y** and **8c** against H5N1 and H5N6 were consistent with their NA-inhibitory potencies and their activities against H5N2 were comparable to OSC. Moreover, it was worth noting that compound **6l** displayed the best inhibition towards all three virus strains, reflecting a great broad-spectrum anti-influenza ability with minimal cytotoxicity and high selectivity index values ($\text{SI} > 400$).

2.2.4 *In silico* prediction of physicochemical properties

An overall assessment of the physicochemical properties of compounds **6g**, **6h**, **6y** and **8z** were further conducted by using free molinspiration software (<http://www.molinspiration.com/>). As depicted in **Table 4**, the results suggested that compounds **6g** and **6l** could theoretically meet the general requirements for useful

drugs, since size, polarity, volume and potentially reactive groups were consistent with the Lipinski's "rule of five" except for the slight deviation of molecular weight of **6l**. However, the parameters of **6y** and **8z**, especially hydrogen bond acceptors (nON) and tPSA, go beyond the normal scope and reflect undesired physicochemical properties. Of note, the topological polar surface area (tPSA), which is characterized by the absorption and membrane permeability of molecules, showed **6g** and **6l** had a value of both 124.17 \AA^2 , confirming their advantage for intestinal absorption ($<140 \text{ \AA}^2$) and inability to penetrate the blood-brain barrier, averting the central nervous system toxicity ($>60 \text{ \AA}^2$) [29].

Table 4. Physicochemical properties of representative compounds

Parameter items	6g	6l	6y	8z
natoms	34	34	35	44
MW (< 500 Da)	489.02	533.47	491.59	616.72
nON (≤ 10)	9	9	12	15
nOHNH (≤ 5)	4	4	4	6
Nrotb (≤ 10)	10	10	10	11
tPSA (<140 \AA^2)	124.17	124.17	153.71	208.50
MV	446.47	451.01	458.84	564.28
miLog p (< 5)	1.5	1.68	-1.53	-0.83
nViol	0	1	2	5

natoms = no. of non-hydrogen atoms; MW= molecular weight; nON = no. of hydrogen bond acceptors; nOHNH = no. of hydrogen bond donors; nrotb = no. of rotatable bonds; tPSA = topological polar surface area; MV = molar volume; miLogP = molinspiration predicted LogP; nViol = number of violations.

2.2.5 *In vivo* anti-influenza activity in Specific Pathogen Free (SPF) chicken embryonated egg

Based on the results of above experiments, in further study, we used an

embryonated egg model which was regarded to have no conflict with ethical and legal aspects of animal protection to test the anti-influenza activity of compound **61** [22, 26, 30]. We infected the embryonated eggs with H5N2 virus and another N2 subtype virus (H9N2) and treated them with injecting different concentrations of **61**. Also, OSC was administrated as control. After 72 h, we recorded the number of the survival and death of the embryonated eggs in **Table 5**. Unexpectedly, as for H5N2 virus, treating with the concentration of 10 mM resulted in 80 % survival (survived/dead = 4/1) of OSC and only 20 % survival (survived/dead = 1/4) of compound **61**, and other lower concentrations had no protective effects for chicken embryos with both tested drugs. By contrast, compound **61** could alleviate mortality in this infection model, as demonstrated by against H9N2 strain. The results clearly showed that the protective potency of **61** for chicken embryos was comparable to OSC at the same concentration with over 80 % survival achieved.

Table 5. Survival number of chick embryos after inoculation of embryonated eggs with influenza virus and administration of **61** or OSC^a.

Virus Strain	Drug	Therapeutic Concentration (mM)	Chick Embryos Survived/ Dead Number
H5N2 ^b	no	Without infection	10/0
	no	Without treatment	0/5
	61	10	1/4
		2.5	0/5
		0.625	0/5
		0.156	0/5
		OSC	10
		2.5	0/5
		0.625	0/5
	0.156	0/5	
H9N2 ^c	no	Without treatment	2/3
	61	10	5/0

	2.5	4/1
	0.625	4/1
	0.156	4/1
OSC	10	5/0
	2.5	5/0
	0.625	4/1
	0.156	3/2

^aThe 200 TCID₅₀ virus solution was mixed with an equal volume of tested compounds and then incubated for 1 h before inoculation.

^bA/Chicken/Hebei/LZF/2014 (H5N2).

^cA/Chicken/China/415/2013 (H9N2).

3. Conclusions

We designed and expeditiously synthesized a series of 1,2,3-triazole oseltamivir derivatives via CuAAC “click reaction” targeting the newly reported 430-cavity. The biological assays demonstrated that the majority of these compounds showed moderate NA inhibition and four compounds (**6g**, **6l**, **6y** and **8c**) showed robust anti-influenza potencies against H5N1, H5N2 and H5N6 strains in both enzymatic assay and cellular assay. Especially, **6l** possessed the most potent and broad-spectrum anti-influenza activity, with IC₅₀ values of 0.12 μM, 0.049 μM and 0.16 μM and EC₅₀ values of 2.45 μM, 4.3 μM and 2.8 μM against H5N1, H5N2 and H5N6 strains, respectively, which were slightly weaker than that of OSC. Besides, molecular modeling revealed that the 1,2,3-triazole linked side chain could extend into the 430-cavity and interact with the amino acid residues around this region in both Group-1 and Group-2 NAs as our original design. More encouragingly, **6l** could achieve the similar protective effect against H9N2 virus with OSC in the embryonated egg model and possessed desirable druglike properties *in silico* prediction. To sum up,

the biological activities and docking studies indicates that the 430-cavity of NA can accommodate various substituents and are worth further exploring for discovering novel and broad-spectrum NAIs.

4. Experimental section

4.1 Chemistry

^1H NMR and ^{13}C NMR spectra were acquired on a Bruker AV-400 spectrometer using d_6 -DMSO and D_2O as solvents. Chemical shifts were reported in δ values (ppm) with TMS as the internal standard, and J values were reported in hertz (Hz). Melting points (mp) were determined on a micromelting point apparatus (Tian Jin Analytical Instrument Factory, Tianjin, China). High-resolution mass spectra (HRMS) were measured using an Agilent 6520 Q-TOF LC/MS spectrometer (Agilent, Germany). Reaction progress was routinely monitored using thin-layer chromatography (TLC) analysis on silica gel GF254, and spots were visualized by irradiation with UV light ($\lambda = 254$ nm). Flash column chromatography was performed on columns packed with silica gel (200-300 mesh), purchased from Qingdao Haiyang Chemical Company. The key reactants oseltamivir phosphate was provided by Shandong Qidu Pharmaceutical. Solvents were of reagent grade and were purified and dried by standard methods when necessary. The solvents of CH_2Cl_2 , THF and MeOH were obtained from Sinopharm Chemical Reagent Co., Ltd (SCRC).

4.1.1 General procedure for the synthesis of compound

ethyl(3*R*,4*R*,5*S*)-4-acetamido-5-((*tert*-butoxycarbonyl)amino)-3-(pentan-3-yloxy)cyclohex-1-ene-1-carboxylate (**2**)

To a solution of commercially available oseltamivir phosphate (**1**) (5 g, 12.2 mmol) in MeOH (50 mL) was added di-*tert*-butoxycarbonyl anhydride ((Boc)₂O, 5 g, 22.3 mmol) and triethylamine (TEA, 2 mL), and the mixture was stirred at room temperature for 12 h. Subsequently, the reaction mixture was transferred to a separator funnel, and the residue was washed with water to afford **2** as a white solid, yield 96.3 %, mp: 149-150 °C.

¹H NMR (400 MHz, DMSO) δ 7.80 (d, *J* = 9.1 Hz, 1H), 6.61 (d, *J* = 6.9 Hz, 2H), 4.21 - 3.99 (m, 3H), 3.75 - 3.61 (m, 1H), 3.57 (td, *J* = 15.6, 10.1 Hz, 1H), 3.38 (dd, *J* = 10.9, 5.5 Hz, 1H), 2.46 (d, *J* = 4.7 Hz, 1H), 2.25 (dd, *J* = 17.5, 10.3 Hz, 1H), 1.78 (s, 3H), 1.52 - 1.28 (m, 13H), 1.22 (t, *J* = 7.1 Hz, 3H), 0.80 (dt, *J* = 26.5, 7.3 Hz, 6H); ¹³C NMR (100 MHz, DMSO) δ 169.66 (s), 165.99 (s), 155.78 (s), 138.66 (s), 129.08 (s), 81.49 (s), 78.04 (s), 75.44 (s), 60.88 (s), 54.61 (s), 49.31 (s), 30.61 (s), 28.65 (s), 26.17 (s), 25.65 (s), 23.31 (s), 14.52 (s), 9.88 (s), 9.43 (s). HRMS: *m/z* 413.2644 [M + H]⁺, C₂₁H₃₆N₂O₆ (412.2573).

4.1.2 General procedure for the synthesis of compound (3*R*, 4*R*, 5*S*)-4-acetamido-5-((*tert*-butoxycarbonyl)amino)-3-(pentan-3-yloxy)cyclohex-1-ene-1-carboxylic acid (**3**)

Intermediate **2** (5 g, 12.1 mmol) was dissolved in 50 mL MeOH, and 4 M NaOH aqueous solution was added until pH to 13. Then the solution was stirred at room

temperature for 2 h. The reaction solution was evaporated under reduced pressure to remove MeOH, and then 3M HCl was added until no more precipitate formed. The precipitate was filtrated and washed with H₂O to afford **3** as white solid, yield 93.3 %, mp: 208-209 °C.

¹H NMR (400 MHz, DMSO) δ 12.55 (s, 1H), 7.81 (d, *J* = 9.1 Hz, 1H), 6.65 - 6.52 (m, 2H), 4.06 (d, *J* = 7.5 Hz, 1H), 3.69 (dd, *J* = 19.4, 9.2 Hz, 1H), 3.56 (dt, *J* = 16.1, 10.2 Hz, 1H), 3.37 (dd, *J* = 11.4, 5.9 Hz, 1H), 2.46 (dd, *J* = 17.9, 4.9 Hz, 1H), 2.21 (dd, *J* = 17.5, 10.3 Hz, 1H), 1.78 (s, 3H), 1.52 - 1.28 (m, 13H), 0.80 (dt, *J* = 26.1, 7.3 Hz, 6H); ¹³C NMR (100 MHz, DMSO) δ 169.71 (s), 167.70 (s), 155.80 (s), 138.13 (s), 129.71 (s), 81.44 (s), 78.04 (s), 75.55 (s), 54.70 (s), 49.44 (s), 30.73 (s), 28.66 (s), 26.19 (s), 25.63 (s), 23.32 (s), 9.89 (s), 9.42 (s). HRMS: *m/z* 385.2338 [M + H]⁺, C₁₉H₃₂N₂O₆ (384.2260).

4.1.3 General procedure for the synthesis of compound **4**.

To a solution of acid **3** (0.38 g, 1mmol), HATU (0.38 g, 1 mmol), and Et₃N (1mL) in 20 mL dry CH₂Cl₂ was added an equimolar amount of the appropriate ynamine (1mmol). The mixture was kept stirring at room temperature for 12 h. After TLC detection to show no starting materials, the mixture was extracted with 100 mL ethyl acetate and washed with saturated NaHCO₃ (3 × 30 mL) and saturated NaCl (1 × 50 mL). The organic layers were dried over MgSO₄, filtered and evaporated under vacuum. The crude product was purified by column chromatography with MeOH:CH₂Cl₂ = 1:30 to obtain intermediate **4**.

4.1.4 General procedure for the synthesis of compound **5**.

The key intermediate **4** (1.0 equiv), azide compounds (1.2 to 1.5 equiv), ascorbic acid sodium (0.6 equiv) and $\text{CuSO}_4 \cdot 5\text{H}_2\text{O}$ (0.3 equiv) were dissolved in the solution of THF/water (V:V= 1:1). The resulting mixture was stirred at room temperature for 6 h. After TLC detection to show no starting materials, 100 mL saturated NaCl was added and the reaction mixture was washed with ethyl acetate (3×50 mL). The combined organic phase was dried over MgSO_4 , filtered, and concentrated under reduced pressure to give the corresponding crude product, which was purified by flash column chromatography $\text{MeOH}:\text{CH}_2\text{Cl}_2 = 1:30$ to afford product **5**.

4.1.5 General procedure for the synthesis of target compounds

The intermediate **5** (0.2 g, about 0.4 mmol) was dissolved in 3 mL MeOH and then 3 mL of 12 M HCl was added. The mixture was stirred at room temperature for 1 h. After TLC detection to show no starting materials, the solvent was evaporated and purified by column chromatography with $\text{MeOH}:\text{CH}_2\text{Cl}_2 = 1:10$ to get target compounds **6a-6z**, **7a-7c** and **8a-8c** as white or pale yellow solid.

(3R,4R,5S)-4-acetamido-5-amino-N-((1-(2-nitrobenzyl)-1H-1,2,3-triazol-4-yl)methyl)-3-(pentan-3-yloxy)cyclohex-1-ene-1-carboxamide (6a): Recrystallized from isopropyl ether as a yellow solid, yield 64 %, mp: 155-156 °C. ^1H NMR (400 MHz,

D₂O) δ 8.03 (dd, $J = 8.2, 1.1$ Hz, 1H), 7.86 (s, 1H), 7.61 (td, $J = 7.6, 1.1$ Hz, 1H), 7.55 - 7.45 (m, 1H), 7.12 (d, $J = 7.6$ Hz, 1H), 6.33 (s, 1H), 5.83 (s, 2H), 4.43 (s, 2H), 4.20 (d, $J = 8.9$ Hz, 1H), 3.96 (dd, $J = 11.7, 9.0$ Hz, 1H), 3.51 (td, $J = 10.8, 5.6$ Hz, 1H), 3.39 (dd, $J = 11.1, 5.6$ Hz, 1H), 2.80 (dd, $J = 16.8, 5.6$ Hz, 1H), 2.54 - 2.39 (m, 1H), 2.00 (s, 3H), 1.38 (dtd, $J = 28.1, 14.2, 7.0$ Hz, 4H), 0.73 (dd, $J = 13.1, 7.3$ Hz, 6H); ¹³C NMR (100 MHz, D₂O) δ 175.23 (s), 168.88 (s), 147.20 (s), 144.63 (s), 134.80 (s), 132.78 (s), 131.03 (s), 130.25 (d, $J = 29.5$ Hz), 130.11 - 129.92 (m), 129.50 (s), 125.54 (s), 124.71 (s), 84.27 (s), 75.07 (s), 52.67 (s), 51.32 (s), 49.13 (s), 34.60 (s), 28.38 (s), 25.42 (s), 25.05 (s), 22.36 (s), 8.47 (s), 8.44 (s). HRMS: m/z 500.2611 [M+H]⁺, C₂₄H₃₃N₇O₅ (499.2543).

(3R,4R,5S)-4-acetamido-5-amino-N-((1-(3-nitrobenzyl)-1H-1,2,3-triazol-4-yl)methyl)-3-(pentan-3-yloxy)cyclohex-1-ene-1-carboxamide (6b): Recrystallized from isopropyl ether as a yellow solid, yield 74 %, mp: 157-160°C. ¹H NMR (400 MHz, D₂O) δ 7.89 (t, $J = 7.7$ Hz, 3H), 7.53 (d, $J = 7.6$ Hz, 1H), 7.38 (t, $J = 7.9$ Hz, 1H), 6.24 (s, 1H), 5.54 (s, 2H), 4.40 (d, $J = 15.9$ Hz, 2H), 4.12 (d, $J = 8.6$ Hz, 1H), 3.89 (dd, $J = 11.5, 9.1$ Hz, 1H), 3.45 (td, $J = 11.0, 5.5$ Hz, 1H), 3.36 - 3.23 (m, 1H), 2.92 - 2.62 (m, 1H), 2.57 - 2.24 (m, 1H), 1.95 (s, 3H), 1.45 - 1.12 (m, 4H), 0.64 (dt, $J = 17.9, 7.4$ Hz, 6H); ¹³C NMR (100 MHz, D₂O) δ 175.19 (s), 168.73 (s), 147.82 (s), 136.55 (s), 134.64 (s), 132.84 (s), 130.28 (s), 130.20 (s), 124.26 (s), 123.49 (s), 122.70 (s), 84.17 (s), 74.97 (s), 52.84 (s), 52.61 (s), 49.08 (s), 34.54 (s), 28.33 (s), 25.37 (s), 25.00 (s), 22.34 (s), 8.46 (s), 8.38 (s). HRMS: m/z 500.2618 [M+H]⁺, C₂₄H₃₃N₇O₅ (499.2543).

(3R,4R,5S)-4-acetamido-5-amino-N-((1-(4-nitrobenzyl)-1H-1,2,3-triazol-4-yl)methyl)-3-(pentan-3-yloxy)cyclohex-1-ene-1-carboxamide (6c): Recrystallized from isopropyl ether as a yellow solid, yield 58 %, mp: 169-171 °C. ¹H NMR (400 MHz, D₂O) δ 7.94 (dd, *J* = 8.0, 3.1 Hz, 3H), 7.29 (d, *J* = 8.2 Hz, 2H), 6.28 (s, 1H), 5.59 (s, 2H), 4.42 (s, 2H), 4.16 (d, *J* = 8.5 Hz, 1H), 3.92 (dd, *J* = 11.6, 9.0 Hz, 1H), 3.49 (td, *J* = 10.9, 5.6 Hz, 1H), 3.43 - 3.26 (m, 1H), 2.78 (dd, *J* = 17.0, 5.2 Hz, 1H), 2.51 - 2.33 (m, 1H), 1.97 (s, 3H), 1.34 (tdt, *J* = 21.5, 14.2, 7.0 Hz, 4H), 0.77 - 0.57 (m, 6H); ¹³C NMR (100 MHz, D₂O) δ 175.21 (s), 168.78 (s), 147.35 (s), 142.10 (s), 132.91 (s), 130.28 (s), 128.78 (s), 124.00 (s), 84.21 (s), 75.00 (s), 53.00 (s), 52.64 (s), 49.10 (s), 34.54 (s), 28.36 (s), 25.40 (s), 25.03 (s), 22.36 (s), 8.48 (s), 8.41 (s). HRMS: *m/z* 500.2611 [M+H]⁺, C₂₄H₃₃N₇O₅ (499.2543).

(3R,4R,5S)-4-acetamido-5-amino-N-((1-(2-fluorobenzyl)-1H-1,2,3-triazol-4-yl)methyl)-3-(pentan-3-yloxy)cyclohex-1-ene-1-carboxamide (6d): Recrystallized from isopropyl ether as a white solid, yield 70 %, mp: 100-102 °C. ¹H NMR (400 MHz, D₂O) δ 7.79 (s, 1H), 7.36 - 7.06 (m, 2H), 6.94 (dt, *J* = 18.6, 8.3 Hz, 2H), 6.24 (s, 1H), 5.40 (s, 2H), 4.12 (d, *J* = 8.4 Hz, 1H), 4.01 - 3.73 (m, 1H), 3.62 - 3.38 (m, 1H), 3.38 - 3.19 (m, 1H), 2.87 - 2.58 (m, 1H), 2.52 - 2.23 (m, 1H), 1.95 (s, 3H), 1.31 (tdt, *J* = 21.3, 14.2, 6.9 Hz, 4H), 0.86 - 0.44 (m, 6H); ¹³C NMR (100 MHz, D₂O) δ 175.20 (s), 168.66 (s), 160.48 (d, ¹*J*_{CF} = 246.7 Hz), 132.90 (s), 131.22 (d, *J* = 8.4 Hz), 130.73 (d, *J* = 3.1 Hz), 130.27 (s), 124.82 (d, *J* = 3.6 Hz), 124.19 (s), 121.42 (d, *J* = 14.8 Hz),

115.74 (s), 115.54 (s), 84.10 (s), 74.97 (s), 52.65 (s), 49.11 (s), 48.03 (s), 34.47 (s), 28.39 (s), 25.41 (s), 25.01 (s), 22.40 (s), 8.48 (s). HRMS: m/z 473.2676 $[M+H]^+$, $C_{24}H_{33}FN_6O_3$ (472.2598).

(3R,4R,5S)-4-acetamido-5-amino-N-((1-(3-fluorobenzyl)-1H-1,2,3-triazol-4-yl)methyl)-3-(pentan-3-yloxy)cyclohex-1-ene-1-carboxamide (6e): Recrystallized from isopropyl ether as a white solid, yield 67 %, mp: 160-162 °C. 1H NMR (400 MHz, D_2O) δ 7.84 (s, 1H), 7.28 (dd, $J = 14.4, 7.5$ Hz, 1H), 6.99 (t, $J = 8.0$ Hz, 2H), 6.92 (d, $J = 9.7$ Hz, 1H), 6.32 (s, 1H), 5.48 (s, 2H), 4.42 (s, 2H), 4.19 (d, $J = 8.9$ Hz, 1H), 3.96 (dd, $J = 11.7, 9.0$ Hz, 1H), 3.51 (td, $J = 10.9, 5.6$ Hz, 1H), 3.43 - 3.32 (m, 1H), 2.79 (dd, $J = 17.1, 5.2$ Hz, 1H), 2.54 - 2.37 (m, 1H), 2.00 (s, 3H), 1.50 - 1.27 (m, 4H), 0.73 (td, $J = 7.4, 4.7$ Hz, 6H); ^{13}C NMR (100 MHz, D_2O) δ 175.23 (s), 168.88 (d, $^1J_{CF} = 245.2$ Hz), 163.84 (s), 161.41 (s), 132.78 (s), 130.84 (d, $J = 8.4$ Hz), 130.37 (s), 123.73 (d, $J = 2.9$ Hz), 115.55 (s), 115.34 (s), 114.81 (s), 114.58 (s), 53.21 (s), 52.64 (s), 49.12 (s), 34.61 (s), 28.35 (s), 25.41 (s), 25.05 (s), 22.35 (s), 8.45 (d, $J = 4.6$ Hz). HRMS: m/z 473.2673 $[M+H]^+$, $C_{24}H_{33}FN_6O_3$ (472.2598).

(3R,4R,5S)-4-acetamido-5-amino-N-((1-(4-fluorobenzyl)-1H-1,2,3-triazol-4-yl)methyl)-3-(pentan-3-yloxy)cyclohex-1-ene-1-carboxamide (6f): Recrystallized from isopropyl ether as a white solid, yield 71 %, mp: 128-130 °C. 1H NMR (400 MHz, D_2O) δ 7.79 (s, 1H), 7.19 (dd, $J = 8.4, 5.5$ Hz, 2H), 6.96 (t, $J = 8.8$ Hz, 2H), 6.28 (s, 1H), 5.41 (s, 2H), 4.37 (s, 2H), 4.16 (d, $J = 8.8$ Hz, 1H), 3.93 (dd, $J = 11.6, 9.1$ Hz,

1H), 3.57 - 3.41 (m, 1H), 3.41 - 3.26 (m, 1H), 2.75 (dd, $J = 17.0, 5.4$ Hz, 1H), 2.52 - 2.33 (m, 1H), 1.97 (s, 3H), 1.36 (tt, $J = 21.1, 7.2$ Hz, 4H), 0.88 - 0.56 (m, 6H); ^{13}C NMR (100 MHz, D_2O) δ 175.20 (s), 168.82 (s), 162.47 (d, $^1 J_{\text{CF}} = 245.0$ Hz), 132.78 (s), 130.63 (d, $J = 3.1$ Hz), 130.31 (s), 130.14 (s), 130.05 (s), 123.87 (s), 115.85 (s), 115.63 (s), 84.27 (s), 75.02 (s), 53.16 (s), 52.61 (s), 49.08 (s), 34.53 (s), 28.32 (s), 25.37 (s), 25.01 (s), 22.32 (s), 8.45 (s), 8.39 (s). HRMS: m/z 473.2672 $[\text{M}+\text{H}]^+$, $\text{C}_{24}\text{H}_{33}\text{FN}_6\text{O}_3$ (472.2598).

(3R,4R,5S)-4-acetamido-5-amino-N-((1-(2-chlorobenzyl)-1H-1,2,3-triazol-4-yl)methyl)-3-(pentan-3-yloxy)cyclohex-1-ene-1-carboxamide (6g): Recrystallized from isopropyl ether as a white solid, yield 73 %, mp: 144-147 °C. ^1H NMR (400 MHz, D_2O) δ 7.82 (s, 1H), 7.33 - 7.10 (m, 4H), 6.28 (s, 1H), 5.53 (s, 2H), 4.40 (s, 2H), 4.17 (d, $J = 8.8$ Hz, 1H), 3.94 (dd, $J = 11.7, 9.0$ Hz, 1H), 3.49 (td, $J = 11.0, 5.6$ Hz, 1H), 3.40 - 3.27 (m, 1H), 2.78 (dd, $J = 16.8, 5.4$ Hz, 1H), 2.53 - 2.38 (m, 1H), 1.99 (s, 3H), 1.46 - 1.26 (m, 4H), 0.72 (tt, $J = 9.7, 4.9$ Hz, 6H); ^{13}C NMR (100 MHz, D_2O) δ 175.23 (s), 168.79 (s), 133.45 (s), 132.78 (s), 131.80 (s), 130.96 (s), 130.62 (s), 130.36 (s), 129.84 (s), 127.65 (s), 124.39 (s), 84.20 (s), 75.01 (s), 52.65 (s), 51.78 (s), 49.10 (s), 34.53 (s), 28.37 (s), 25.42 (s), 25.04 (s), 22.36 (s), 8.47 (s). HRMS: m/z 489.2379 $[\text{M}+\text{H}]^+$, $\text{C}_{24}\text{H}_{33}\text{ClN}_6\text{O}_3$ (488.2303). HPLC purity: 99.99%.

(3R,4R,5S)-4-acetamido-5-amino-N-((1-(3-chlorobenzyl)-1H-1,2,3-triazol-4-yl)methyl)-3-(pentan-3-yloxy)cyclohex-1-ene-1-carboxamide (6h): Recrystallized from

isopropyl ether as a white solid, yield 70 %, mp: 150-152 °C. ^1H NMR (400 MHz, D_2O) δ 7.81 (s, 1H), 7.31 - 6.95 (m, 4H), 6.26 (s, 1H), 5.41 (s, 2H), 4.38 (s, 2H), 4.13 (d, $J = 8.1$ Hz, 1H), 3.98 - 3.83 (m, 1H), 3.46 (td, $J = 10.9, 5.6$ Hz, 1H), 3.37 - 3.23 (m, 1H), 2.84 - 2.67 (m, 1H), 2.52 - 2.33 (m, 1H), 1.96 (s, 3H), 1.47 - 1.18 (m, 4H), 0.68 (dd, $J = 17.3, 7.4$ Hz, 6H); ^{13}C NMR (100 MHz, D_2O) δ 175.20 (s), 168.78 (s), 136.66 (s), 134.05 (s), 132.76 (s), 130.40 (d, $J = 12.8$ Hz), 128.61 (s), 127.77 (s), 126.35 (s), 124.05 (s), 84.17 (s), 74.97 (s), 53.15 (s), 52.61 (s), 49.08 (s), 34.55 (s), 28.33 (s), 25.38 (s), 25.00 (s), 22.32 (s), 8.51 (s). HRMS: 489.2374 $[\text{M}+\text{H}]^+$, $\text{C}_{24}\text{H}_{33}\text{ClN}_6\text{O}_3$ (488.2303).

(3R,4R,5S)-4-acetamido-5-amino-N-((1-(4-chlorobenzyl)-1H-1,2,3-triazol-4-yl)methyl)-3-(pentan-3-yloxy)cyclohex-1-ene-1-carboxamide (6i): Recrystallized from isopropyl ether as a white solid, yield 74 %, mp: 135-137 °C. ^1H NMR (400 MHz, D_2O) δ 7.81 (s, 1H), 7.30 - 6.99 (m, 4H), 6.26 (s, 1H), 5.40 (s, 2H), 4.38 (s, 2H), 4.23 - 4.07 (m, 1H), 4.01 - 3.83 (m, 1H), 3.46 (td, $J = 10.9, 5.6$ Hz, 1H), 3.39 - 3.23 (m, 1H), 2.75 (dd, $J = 16.5, 4.5$ Hz, 1H), 2.57 - 2.30 (m, 1H), 1.96 (s, 3H), 1.51 - 1.18 (m, 4H), 0.86 - 0.48 (m, 6H); ^{13}C NMR (100 MHz, D_2O) δ 175.22 (s), 168.79 (s), 144.72 (s), 133.89 (s), 133.35 (s), 132.79 (s), 130.33 (s), 129.56 (s), 128.95 (s), 123.97 (s), 84.22 (s), 75.00 (s), 53.16 (s), 52.63 (s), 49.09 (s), 34.54 (s), 28.34 (s), 25.40 (s), 25.03 (s), 22.34 (s), 8.46 (s, $J = 2.6$ Hz), 8.44 (s). HRMS: m/z 489.2376 $[\text{M}+\text{H}]^+$, $\text{C}_{24}\text{H}_{33}\text{ClN}_6\text{O}_3$ (488.2303).

(3R,4R,5S)-4-acetamido-5-amino-N-((1-(2-bromobenzyl)-1H-1,2,3-triazol-4-yl)methyl)-3-(pentan-3-yloxy)cyclohex-1-ene-1-carboxamide (6j): Recrystallized from isopropyl ether as a pale yellow solid, yield 74 %, mp: 162-163 °C. ¹H NMR (400 MHz, MeOD) δ 8.27 (s, 1H), 7.69 (d, *J* = 8.1 Hz, 1H), 7.42 (t, *J* = 7.2 Hz, 1H), 7.33 (s, 2H), 6.54 (s, 1H), 5.79 (s, 2H), 4.57 (s, 2H), 4.27 (d, *J* = 7.6 Hz, 1H), 4.11 - 3.88 (m, 1H), 3.54 (s, 1H), 3.50 - 3.43 (m, 1H), 2.90 (d, *J* = 16.1 Hz, 1H), 2.52 (s, 1H), 2.06 (s, 3H), 1.54 (ddt, *J* = 21.1, 14.0, 6.8 Hz, 4H), 0.91 (q, *J* = 6.9 Hz, 6H); ¹³C NMR (100 MHz, MeOD) δ 188.57 (s), 173.38 (s), 133.77 (s), 133.02 (s), 132.52 (s), 131.32 - 130.89 (m), 130.66 (d, *J* = 25.7 Hz), 128.02 (s), 123.40 (s), 82.34 (s), 74.23 (s), 54.40 (s), 53.03 (s), 49.49 (s), 34.21 (s), 28.35 (s), 25.76 (s), 25.10 (s), 21.80 (s), 8.39 (s), 8.16 (s). HRMS: *m/z* 533.1875 [M+H]⁺, C₂₄H₃₃BrN₆O₃ (532.1798).

(3R,4R,5S)-4-acetamido-5-amino-N-((1-(3-bromobenzyl)-1H-1,2,3-triazol-4-yl)methyl)-3-(pentan-3-yloxy)cyclohex-1-ene-1-carboxamide (6k): Recrystallized from isopropyl ether as a pale yellow solid, yield 77 %, mp: 155-157 °C. ¹H NMR (400 MHz, D₂O) δ 7.79 (s, 1H), 7.19 (d, *J* = 12.4 Hz, 2H), 7.07 (d, *J* = 7.4 Hz, 1H), 7.00 (t, *J* = 7.7 Hz, 1H), 6.22 (s, 1H), 5.33 (s, 2H), 4.35 (s, 2H), 4.10 (d, *J* = 8.3 Hz, 1H), 4.02 - 3.78 (m, 1H), 3.45 (td, *J* = 11.0, 5.7 Hz, 1H), 3.33 - 3.17 (m, 1H), 2.75 (dd, *J* = 17.0, 4.7 Hz, 1H), 2.54 - 2.29 (m, 1H), 1.87 (d, *J* = 65.3 Hz, 3H), 1.42 - 1.08 (m, 4H), 0.66 (tt, *J* = 22.4, 7.1 Hz, 6H); ¹³C NMR (100 MHz, D₂O) δ 175.15 (s), 168.58 (s), 136.88 (s), 132.84 (s), 131.52 (s), 130.73 (s), 130.69 (s), 130.29 (s), 126.92 (s), 124.01 (s), 122.24 (s), 83.93 (s), 74.89 (s), 53.09 (s), 52.64 (s), 49.07 (s), 34.52 (s), 28.40 (s),

25.43 (s), 24.99 (s), 22.36 (s), 8.56 (s), 8.47 (s). HRMS: m/z 533.1885 $[M+H]^+$, $C_{24}H_{33}BrN_6O_3$ (532.1798).

(3R,4R,5S)-4-acetamido-5-amino-N-((1-(4-bromobenzyl)-1H-1,2,3-triazol-4-yl)methyl)-3-(pentan-3-yloxy)cyclohex-1-ene-1-carboxamide (6l): Recrystallized from isopropyl ether as a pale yellow solid, yield 77 %, mp: 148-150 °C. 1H NMR (400 MHz, D_2O) δ 7.84 (s, 1H), 7.24 (d, J = 8.2 Hz, 2H), 7.02 (d, J = 2.9 Hz, 2H), 6.25 (s, 1H), 5.37 (s, 2H), 4.39 (s, 2H), 4.14 (d, J = 8.7 Hz, 1H), 3.98 - 3.84 (m, 1H), 3.48 (td, J = 11.0, 5.6 Hz, 1H), 3.30 (s, 1H), 2.82 - 2.70 (m, 1H), 2.45 (dd, J = 15.0, 12.3 Hz, 1H), 1.98 (s, 3H), 1.43 - 1.19 (m, 4H), 0.75 - 0.54 (m, 6H); ^{13}C NMR (100 MHz, DMSO) δ 171.03 (s), 166.40 (s), 145.74 (s), 136.02 (s), 132.50 (s), 132.12 (s), 130.73 (s), 130.70 (s), 123.60 (s), 121.85 (s), 81.53 (s), 74.69 (s), 52.95 (s), 52.41 (s), 49.58 (s), 34.95 (s), 29.10 (s), 26.13 (s), 25.40 (s), 23.82 (s), 9.84 (s), 9.38 (s). HRMS: m/z 533.1874 $[M+H]^+$, $C_{24}H_{33}BrN_6O_3$ (532.1798). HPLC purity: 96.52%.

(3R,4R,5S)-4-acetamido-5-amino-N-((1-benzyl-1H-1,2,3-triazol-4-yl)methyl)-3-(pentan-3-yloxy)cyclohex-1-ene-1-carboxamide (6m): Recrystallized from isopropyl ether as a white solid, yield 90 %, mp: 145-146 °C. 1H NMR (400 MHz, D_2O) δ 7.85 (s, 1H), 7.34 - 7.09 (m, 5H), 6.31 (s, 1H), 5.46 (s, 2H), 4.40 (s, 2H), 4.18 (d, J = 9.0 Hz, 1H), 3.94 (dd, J = 11.7, 9.0 Hz, 1H), 3.49 (td, J = 11.0, 5.6 Hz, 1H), 3.38 (p, J = 5.5 Hz, 1H), 2.77 (dd, J = 16.9, 5.3 Hz, 1H), 2.54 - 2.38 (m, 1H), 1.98 (s, 3H), 1.37

(ddd, $J = 21.1, 13.6, 6.7$ Hz, 4H), 0.72 (td, $J = 7.3, 1.6$ Hz, 6H); ^{13}C NMR (100 MHz, D_2O) δ 175.23 (s), 169.05 - 168.85 (m), 134.62 (s), 132.85 (s), 130.32 (s), 129.11 (s), 128.78 (s), 128.05 (s), 84.29 (s), 75.05 (s), 54.06 (s), 52.63 (s), 49.11 (s), 34.51 (s), 28.34 (s), 25.41 (s), 25.04 (s), 22.36 (s), 8.46 (s), 8.44 (s). HRMS: m/z 455.2761 $[\text{M}+\text{H}]^+$. $\text{C}_{24}\text{H}_{34}\text{N}_6\text{O}_3$ (454.2692).

(3R,4R,5S)-4-acetamido-5-amino-3-(pentan-3-yloxy)-N-((1-phenethyl-1H-1,2,3-triazol-4-yl)methyl)cyclohex-1-ene-1-carboxamide (6n): Recrystallized from isopropyl ether as a white solid, yield 81 %, mp: 145-147 °C. ^1H NMR (400 MHz, D_2O) δ 7.51 (s, 1H), 7.23 - 7.05 (m, 3H), 7.00 - 6.82 (m, 2H), 6.31 (s, 1H), 4.57 (t, $J = 6.5$ Hz, 2H), 4.32 (s, 2H), 4.23 (d, $J = 8.7$ Hz, 1H), 3.97 (dd, $J = 11.6, 9.1$ Hz, 1H), 3.52 (td, $J = 11.0, 5.6$ Hz, 1H), 3.47 - 3.35 (m, 1H), 3.06 (t, $J = 6.5$ Hz, 2H), 2.77 (dd, $J = 16.9, 5.3$ Hz, 1H), 2.54 - 2.37 (m, 1H), 1.99 (s, 3H), 1.52 - 1.28 (m, 4H), 0.75 (dd, $J = 16.0, 7.6$ Hz, 6H); ^{13}C NMR (100 MHz, D_2O) δ 175.26 (s), 168.61 (s), 137.24 (s), 132.91 (s), 130.25 (s), 128.69 (d, $J = 4.6$ Hz), 126.91 (s), 124.66 (s), 84.28 (s), 75.06 (s), 52.69 (s), 52.03 (s), 49.15 (s), 35.66 (s), 34.20 (s), 28.37 (s), 25.48 (s), 25.06 (s), 22.38 (s), 8.55 (s), 8.47 (s). HRMS: m/z 469.2927 $[\text{M}+\text{H}]^+$, $\text{C}_{25}\text{H}_{36}\text{N}_6\text{O}_3$ (468.2849).

(3R,4R,5S)-4-acetamido-5-amino-N-((1-(4-chloro-3-fluorobenzyl)-1H-1,2,3-triazol-4-yl)methyl)-3-(pentan-3-yloxy)cyclohex-1-ene-1-carboxamide (6o): Recrystallized from isopropyl ether as a white solid, yield 81 %, mp: 117-118 °C. ^1H NMR (400 MHz, D_2O) δ 7.79 (d, $J = 14.0$ Hz, 1H), 7.17 (t, $J = 7.9$ Hz, 1H), 6.91 (dd,

$J = 20.9, 9.1$ Hz, 2H), 6.30 (d, $J = 61.3$ Hz, 1H), 5.38 (s, 2H), 4.35 (s, 2H), 4.10 (d, $J = 8.0$ Hz, 1H), 3.96 - 3.78 (m, 1H), 3.43 (dd, $J = 16.1, 10.9$ Hz, 1H), 3.35 - 3.17 (m, 1H), 2.73 (dd, $J = 18.5, 5.5$ Hz, 1H), 2.48 - 2.31 (m, 1H), 1.93 (s, 3H), 1.40 - 1.12 (m, 4H), 0.80 - 0.46 (m, 6H); ^{13}C NMR (100 MHz, D_2O) δ 175.19 (s), 168.75 (s), 157.56 (d, $^1J_{\text{CF}} = 247.7$ Hz), 135.64 (d, $J = 6.9$ Hz), 132.78 (s), 130.96 (s), 130.33 (s), 124.71 (d, $J = 3.5$ Hz), 120.52 (s), 120.32 (s), 116.20 (s), 115.98 (s), 84.15 (s), 74.95 (s), 52.67 (d, $J = 8.5$ Hz), 49.08 (s), 34.53 (s), 28.34 (s), 25.38 (s), 25.00 (s), 22.33 (s), 8.45 (s), 8.40 (s). HRMS: m/z 507.2285.2 $[\text{M}+\text{H}]^+$, $\text{C}_{24}\text{H}_{32}\text{ClFN}_6\text{O}_3$ (506.2208).

(3R,4R,5S)-4-acetamido-5-amino-N-((1-(2-chloro-4-fluorobenzyl)-1H-1,2,3-triazol-4-yl)methyl)-3-(pentan-3-yloxy)cyclohex-1-ene-1-carboxamide (6p):

Recrystallized from isopropyl ether as a white solid, yield 78 %, mp: 160-162 °C. ^1H NMR (400 MHz, D_2O) δ 7.79 (s, 1H), 7.34 - 7.16 (m, 1H), 7.18 - 7.03 (m, 1H), 6.94 (t, $J = 7.4$ Hz, 1H), 6.25 (s, 1H), 5.50 (s, 2H), 4.46 - 4.26 (m, 2H), 4.14 (d, $J = 8.3$ Hz, 1H), 3.93 (dd, $J = 25.8, 14.4$ Hz, 1H), 3.46 (td, $J = 11.1, 5.6$ Hz, 1H), 3.40 - 3.22 (m, 1H), 2.72 (d, $J = 4.4$ Hz, 1H), 2.57 - 2.27 (m, 1H), 1.95 (s, 3H), 1.55 - 1.10 (m, 4H), 0.68 (dd, $J = 14.4, 7.2$ Hz, 6H); ^{13}C NMR (100 MHz, D_2O) δ 175.22 (s), 168.83 (s), 162.45 (d, $^1J_{\text{CF}} = 249.3$ Hz), 144.50 (s), 134.56 (s), 132.73 (s), 132.45 (d, $J = 9.4$ Hz), 130.38 (s), 128.09 (s), 124.23 (s), 117.28 (s), 117.03 (s), 84.26 (s), 75.02 (s), 52.62 (s), 51.11 (s), 49.09 (s), 34.53 (s), 28.34 (s), 25.39 (s), 25.02 (s), 22.32 (s), 8.45 (s), 8.41 (s). HRMS: m/z 507.2284 $[\text{M}+\text{H}]^+$, $\text{C}_{24}\text{H}_{32}\text{ClFN}_6\text{O}_3$ (506.2208).

(3R,4R,5S)-4-acetamido-5-amino-N-((1-(4-cyanobenzyl)-1H-1,2,3-triazol-4-yl)methyl)-3-(pentan-3-yloxy)cyclohex-1-ene-1-carboxamide (6q): Recrystallized from isopropyl ether as a white solid, yield 87 %, mp: 128-130 °C. ¹H NMR (400 MHz, D₂O) δ 7.84 (s, 1H), 7.56 (d, *J* = 8.2 Hz, 2H), 7.27 (t, *J* = 12.1 Hz, 2H), 6.28 (s, 1H), 5.54 (s, 2H), 4.46 - 4.28 (m, 2H), 4.15 (d, *J* = 8.7 Hz, 1H), 3.92 (dd, *J* = 11.6, 9.0 Hz, 1H), 3.47 (td, *J* = 11.0, 5.6 Hz, 1H), 3.41 - 3.28 (m, 1H), 2.75 (dd, *J* = 17.6, 6.1 Hz, 1H), 2.51 - 2.29 (m, 1H), 1.95 (s, 3H), 1.48 - 1.21 (m, 4H), 0.83 - 0.48 (m, 6H); ¹³C NMR (100 MHz, D₂O) δ 175.22 (s), 168.88 (s), 144.89 (s), 140.31 (s), 132.98 (s), 132.80 (s), 130.36 (s), 128.38 (s), 124.25 (s), 119.11 (s), 111.12 (s), 84.31 (s), 75.05 (s), 53.22 (s), 52.62 (s), 49.10 (s), 34.59 (s), 28.33 (s), 25.39 (s), 25.04 (s), 22.32 (s), 8.46 (s), 8.40 (s). HRMS: *m/z* 480.2717 [M+H]⁺, C₂₅H₃₃N₇O₃ (479.2645).

(3R,4R,5S)-4-acetamido-5-amino-N-((1-(4-methylbenzyl)-1H-1,2,3-triazol-4-yl)methyl)-3-(pentan-3-yloxy)cyclohex-1-ene-1-carboxamide (6r): Recrystallized from isopropyl ether as a white solid, yield 69 %, mp: 130-132 °C. ¹H NMR (400 MHz, D₂O) δ 7.44 (s, 1H), 6.71 (s, 4H), 5.94 (s, 1H), 5.01 (s, 2H), 4.03 (s, 2H), 3.83 (d, *J* = 7.1 Hz, 1H), 3.71 - 3.45 (m, 1H), 3.15 (s, 1H), 3.02 (s, 1H), 2.43 (d, *J* = 15.7 Hz, 1H), 2.25 - 1.98 (m, 1H), 1.79 (s, 3H), 1.65 (s, 3H), 1.21 - 0.85 (m, 4H), 0.59 - 0.21 (m, 6H); ¹³C NMR (100 MHz, D₂O) δ 175.20 (s), 168.90 (s), 138.96 (s), 132.78 (s), 131.63 (s), 130.31 (s), 129.57 (s), 128.05 (s), 123.79 (s), 84.14 (s), 74.95 (s), 53.66 (s), 52.62 (s), 49.06 (s), 34.50 (s), 28.33 (s), 25.37 (s), 24.99 (s), 22.33 (s), 20.14 (s), 8.43 (s). HRMS: *m/z* 469.2717 [M+H]⁺, C₂₅H₃₆N₆O₃ (468.2849).

(3R,4R,5S)-N-((1-([1,1'-biphenyl]-4-ylmethyl)-1H-1,2,3-triazol-4-yl)methyl)-4-acetamido-5-amino-3-(pentan-3-yloxy)cyclohex-1-ene-1-carboxamide (6s): Recrystallized from isopropyl ether as a white solid, yield 50 %, mp: 168-171 °C. ¹H NMR (400 MHz, MeOD) δ 8.11 (s, 1H), 7.64 (dd, *J* = 15.5, 7.7 Hz, 4H), 7.45 (d, *J* = 5.0 Hz, 4H), 7.36 (t, *J* = 7.2 Hz, 1H), 6.52 (s, 1H), 5.68 (s, 2H), 4.54 (s, 2H), 4.24 (d, *J* = 8.3 Hz, 1H), 3.98 (dd, *J* = 24.6, 14.2 Hz, 1H), 3.51 (s, 1H), 3.49 - 3.41 (m, 1H), 2.87 (d, *J* = 12.7 Hz, 1H), 2.51 (d, *J* = 10.1 Hz, 1H), 2.05 (s, 3H), 1.53 (ddd, *J* = 21.0, 13.9, 7.1 Hz, 4H), 0.90 (t, *J* = 6.3 Hz, 6H); ¹³C NMR (100 MHz, DMSO) δ 171.03 (s), 166.40 (s), 140.48 (s), 140.06 (s), 135.73 (s), 132.50 (s), 130.71 (s), 129.42 (s), 129.14 (s), 128.08 (s), 127.51 (s), 127.18 (s), 123.60 (s), 81.53 (s), 74.69 (s), 52.95 (s), 52.88 (s), 49.59 (s), 34.98 (s), 29.11 (s), 26.13 (s), 25.39 (s), 23.82 (s), 9.84 (s), 9.38 (s). HRMS: *m/z* 531.3081 [M+H]⁺, C₃₀H₃₈N₆O₃ (530.3005).

(3R,4R,5S)-4-acetamido-5-amino-N-((1-(naphthalen-2-ylmethyl)-1H-1,2,3-triazol-4-yl)methyl)-3-(pentan-3-yloxy)cyclohex-1-ene-1-carboxamide (6t): Recrystallized from isopropyl ether as a white solid, yield 46 %, mp: 158-160 °C. ¹H NMR (400 MHz, D₂O) δ 7.56 (s, 1H), 6.95 (ddd, *J* = 20.6, 18.6, 12.7 Hz, 7H), 6.01 (s, 1H), 5.06 (s, 2H), 4.18 (d, *J* = 49.9 Hz, 2H), 4.04 - 3.72 (m, 2H), 3.36 (d, *J* = 5.8 Hz, 1H), 2.89 (d, *J* = 20.1 Hz, 1H), 2.71 (d, *J* = 8.0 Hz, 1H), 2.39 (s, 1H), 1.96 (d, *J* = 17.6 Hz, 3H), 1.24 - 0.77 (m, 4H), 0.40 (dt, *J* = 82.4, 6.8 Hz, 6H); ¹³C NMR (100 MHz, D₂O) δ 174.96 (s), 168.09 (s), 132.92 (s), 132.66 (s), 132.46 (s), 132.08 (s), 130.08 (s),

128.45 (s), 127.69 (s), 127.29 (s), 127.08 (s), 126.21 (s), 125.29 (s), 83.15 (s), 74.65 (s), 53.64 (s), 52.63 (s), 49.01 (s), 34.48 (s), 28.48 (s), 25.31 (s), 24.88 (s), 22.45 (s), 8.50 (s), 8.41 (s). HRMS: m/z 505.2921 $[M+H]^+$, $C_{28}H_{36}N_6O_3$ (504.2849).

(3R,4R,5S)-4-acetamido-5-amino-3-(pentan-3-yloxy)-N-((1-((phenylthio)methyl)-1H-1,2,3-triazol-4-yl)methyl)cyclohex-1-ene-1-carboxamide (6u): Recrystallized from isopropyl ether as a white solid, yield 41 %, mp: 155-158 °C. 1H NMR (400 MHz, D_2O) δ 7.62 (s, 1H), 7.48 - 6.95 (m, 5H), 6.33 (s, 1H), 5.64 (d, $J = 38.1$ Hz, 2H), 4.34 (s, 2H), 4.22 (t, $J = 13.4$ Hz, 1H), 4.09 - 3.92 (m, 1H), 3.54 (td, $J = 11.0, 5.6$ Hz, 1H), 3.46 - 3.30 (m, 1H), 2.81 (dd, $J = 16.9, 4.9$ Hz, 1H), 2.61 - 2.39 (m, 1H), 2.03 (s, 3H), 1.40 (ddd, $J = 21.1, 13.5, 6.7$ Hz, 4H), 0.77 (t, $J = 6.9$ Hz, 6H); ^{13}C NMR (100 MHz, D_2O) δ 175.23 (s), 168.52 (s), 144.74 (s), 133.31 (s), 132.87 (s), 130.69 - 130.54 (m), 130.40 (s), 129.47 (s), 129.15 (s), 123.75 (s), 84.19 (s), 75.01 (s), 53.89 (s), 52.70 (s), 49.14 (s), 34.45 (s), 28.40 (s), 25.49 (s), 25.05 (s), 22.38 (s), 8.59 (s), 8.49 (s). HRMS: m/z 487.2486 $[M+H]^+$, $C_{24}H_{34}N_6O_3S$ (486.2413).

(3R,4R,5S)-4-acetamido-5-amino-N-((1-(4-bromophenethyl)-1H-1,2,3-triazol-4-yl)methyl)-3-(pentan-3-yloxy)cyclohex-1-ene-1-carboxamide (6v): Recrystallized from isopropyl ether as a white solid, yield 72 %, mp: 150-152 °C. 1H NMR (400 MHz, D_2O) δ 7.41 (s, 1H), 7.14 (d, $J = 7.5$ Hz, 2H), 6.71 (d, $J = 7.8$ Hz, 2H), 6.25 (s, 1H), 4.43 (s, 2H), 4.27 (s, 2H), 4.19 (d, $J = 7.3$ Hz, 1H), 4.11 - 3.81 (m, 1H), 3.65 - 3.44 (m, 1H), 3.34 (s, 1H), 2.90 (d, $J = 18.6$ Hz, 2H), 2.77 (d, $J = 12.4$ Hz, 1H), 2.60 -

2.31 (m, 1H), 1.96 (s, 3H), 1.27 (dd, $J = 37.8, 30.7$ Hz, 4H), 0.68 (d, $J = 3.9$ Hz, 6H); ^{13}C NMR (100 MHz, D_2O) δ 175.19 (s), 168.41 (s), 144.25 (s), 136.45 (s), 132.80 (s), 131.39 (s), 130.59 (s), 130.36 (s), 124.21 (s), 120.15 (s), 84.01 (s), 74.97 (s), 51.31 (s), 49.16 (s), 35.19 (s), 34.39 (s), 28.46 (s), 25.55 (s), 25.09 (s), 22.40 (s), 8.67 (s, $J = 13.7$ Hz), 8.53 (s). HRMS: m/z 547.2032 $[\text{M}+\text{H}]^+$, $\text{C}_{25}\text{H}_{35}\text{BrN}_6\text{O}_3$ (546.1954).

(3R,4R,5S)-4-acetamido-5-amino-N-((1-cyclohexyl-1H-1,2,3-triazol-4-yl)methyl)-3-(pentan-3-yloxy)cyclohex-1-ene-1-carboxamide (6w): Recrystallized from isopropyl ether as a white solid, yield 33 %, mp: 165-168 °C. ^1H NMR (400 MHz, D_2O) δ 7.88 (s, 1H), 6.32 (s, 1H), 4.38 (s, 3H), 4.16 (s, 1H), 3.99 - 3.81 (m, 1H), 3.46 (s, 1H), 3.37 (s, 1H), 2.74 (d, $J = 13.5$ Hz, 1H), 2.47 (d, $J = 34.6$ Hz, 1H), 1.93 (s, 5H), 1.71 (d, $J = 10.6$ Hz, 2H), 1.59 (d, $J = 12.4$ Hz, 3H), 1.46 - 1.20 (m, 6H), 1.10 (d, $J = 11.2$ Hz, 1H), 0.69 (d, $J = 7.5$ Hz, 6H); ^{13}C NMR (100 MHz, D_2O) δ 175.20 (s), 168.94 (s), 132.98 (s), 130.22 (s), 122.58 (s), 84.37 (s), 75.07 (s), 61.26 (s), 52.60 (s), 49.08 (s), 47.08 (s), 34.25 (s), 32.63 (s), 28.31 (s), 25.38 (s), 25.01 (s), 24.49 (s), 22.31 (s), 8.44 (s), 8.41 (s). HRMS: m/z 447.3083 $[\text{M}+\text{H}]^+$, $\text{C}_{23}\text{H}_{38}\text{N}_6\text{O}_3$ (446.3005).

(3R,4R,5S)-4-acetamido-5-amino-N-((1-(2-oxo-2-(pyrrolidin-1-yl)ethyl)-1H-1,2,3-triazol-4-yl)methyl)-3-(pentan-3-yloxy)cyclohex-1-ene-1-carboxamide(6x):

Recrystallized from isopropyl ether as a white solid, yield 43 %, mp: 136-138 °C. ^1H NMR (400 MHz, D_2O) δ 7.81 (s, 1H), 6.35 (s, 1H), 5.28 (s, 2H), 4.43 (s, 2H), 4.20 (d, $J = 8.5$ Hz, 1H), 3.94 (dd, $J = 11.5, 9.1$ Hz, 1H), 3.52 - 3.37 (m, 4H), 3.31 (t, $J = 6.8$

Hz, 2H), 2.77 (dd, $J = 16.8, 5.2$ Hz, 1H), 2.51 - 2.40 (m, 1H), 1.96 (s, 3H), 1.88 (dd, $J = 13.3, 6.7$ Hz, 2H), 1.82 - 1.72 (m, 2H), 1.48 - 1.24 (m, 4H), 0.72 (dt, $J = 11.2, 7.4$ Hz, 6H); ^{13}C NMR (100 MHz, D_2O) δ 175.20 (s), 168.68 (d, $J = 47.2$ Hz), 168.35 - 168.23 (m), 165.39 (s), 132.93 (s), 130.27 (s), 125.59 (d, $J = 6.4$ Hz), 84.34 (s), 75.09 (s), 52.60 (s), 51.63 (s), 49.11 (s), 46.62 (s), 46.37 (s), 34.57 (s), 28.34 (s), 25.39 (d, $J = 4.8$ Hz), 25.01 (s), 23.63 (s), 22.35 (s), 8.45 (s). HRMS: m/z 476.2982 $[\text{M}+\text{H}]^+$, $\text{C}_{23}\text{H}_{37}\text{N}_7\text{O}_4$ (475.2907).

(3R,4R,5S)-4-acetamido-5-amino-N-((1-(2-morpholino-2-oxoethyl)-1H-1,2,3-triazol-4-yl)methyl)-3-(pentan-3-yloxy)cyclohex-1-ene-1-carboxamide (6y): Recrystallized from isopropyl ether as a white solid, yield 56%, mp: 129-131 °C. ^1H NMR (400 MHz, D_2O) δ 7.82 (s, 1H), 6.35 (s, 1H), 5.43 (s, 2H), 4.44 (s, 2H), 4.20 (d, $J = 8.7$ Hz, 1H), 3.95 (dd, $J = 11.6, 9.0$ Hz, 1H), 3.75 - 3.66 (m, 2H), 3.62 (dd, $J = 11.3, 6.2$ Hz, 2H), 3.57 - 3.44 (m, 5H), 3.40 (dd, $J = 11.0, 5.5$ Hz, 1H), 2.77 (dt, $J = 17.2, 8.6$ Hz, 1H), 2.55 - 2.30 (m, 1H), 1.96 (s, 3H), 1.48 - 1.26 (m, 4H), 0.72 (dt, $J = 11.2, 7.4$ Hz, 6H); ^{13}C NMR (100 MHz, D_2O) δ 175.20 (s), 168.89 (s), 165.88 (s), 132.98 (s), 130.24 (s), 125.77 (s), 84.33 (s), 75.09 (s), 66.11 (s), 65.90 (s), 52.61 (s), 51.14 (s), 49.12 (s), 45.16 (s), 42.53 (s), 34.51 (s), 28.35 (s), 25.42 (s), 25.02 (s), 22.38 (s), 8.47 (s). HRMS: m/z 492.2934 $[\text{M}+\text{H}]^+$, $\text{C}_{23}\text{H}_{37}\text{N}_7\text{O}_5$ (491.2856). HPLC purity: 95.59%.

(3R,4R,5S)-4-acetamido-5-amino-N-((1-(2-(hydroxymethyl)-5-(5-methyl-2,4-dioxo-3,4-dihydropyrimidin-1(2H)-yl)tetrahydrofuran-3-yl)-1H-1,2,3-triazol-4-yl)met

hyl)-3-(pentan-3-yloxy)cyclohex-1-ene-1-carboxamide (6z): Recrystallized from isopropyl ether as a white solid, yield 40 %, mp: 198-200 °C. ¹H NMR (400 MHz, D₂O) δ 7.94 (s, 1H), 7.63 (s, 1H), 6.45 - 6.25 (m, 2H), 5.30 (dd, *J* = 14.3, 5.8 Hz, 1H), 4.42 (s, 2H), 4.34 (d, *J* = 5.1 Hz, 1H), 4.20 (d, *J* = 8.7 Hz, 1H), 3.95 (dd, *J* = 11.5, 9.1 Hz, 1H), 3.78 (dd, *J* = 12.7, 3.1 Hz, 1H), 3.68 (dd, *J* = 12.7, 4.2 Hz, 1H), 3.48 (dd, *J* = 11.2, 5.7 Hz, 1H), 3.40 (d, *J* = 5.4 Hz, 1H), 2.93 - 2.62 (m, 3H), 2.46 (dd, *J* = 15.2, 12.2 Hz, 1H), 1.96 (s, 3H), 1.79 (s, 3H), 1.36 (ddd, *J* = 21.4, 13.6, 6.9 Hz, 4H), 0.73 (dt, *J* = 10.1, 7.4 Hz, 6H); ¹³C NMR (100 MHz, D₂O) δ 175.21 (s), 168.94 (s), 166.47 (s), 151.53 (s), 137.68 (s), 132.86 (s), 130.31 (s), 123.34 (s), 85.47 (s), 84.38 (s), 84.20 (s), 75.08 (s), 60.49 (s), 59.54 (s), 52.61 (s), 49.10 (s), 36.83 (s), 34.62 (s), 28.33 (s), 25.39 (s), 25.01 (s), 22.31 (s), 11.50 (s), 8.45 (s), 8.41 (s). HRMS: *m/z* 589.3093 [M+H]⁺, C₂₇H₄₀N₈O₇ (588.3020).

(3R,4R,5S)-4-acetamido-5-amino-N-(2-(1-(4-nitrobenzyl)-1H-1,2,3-triazol-4-yl)ethyl)-3-(pentan-3-yloxy)cyclohex-1-ene-1-carboxamide (7a): Recrystallized from isopropyl ether as a white solid, yield 67 %, mp: 120-123 °C. ¹H NMR (400 MHz, D₂O) δ 7.75 (d, *J* = 8.5 Hz, 2H), 7.57 (s, 1H), 6.99 (d, *J* = 8.5 Hz, 2H), 5.73 (s, 1H), 5.32 (s, 2H), 3.79 (d, *J* = 8.6 Hz, 1H), 3.64 - 3.50 (m, 1H), 3.15 (dd, *J* = 15.5, 10.0 Hz, 3H), 2.97 (dd, *J* = 15.3, 9.9 Hz, 1H), 2.57 (t, *J* = 5.9 Hz, 2H), 2.45 - 2.31 (m, 1H), 2.09 (dd, *J* = 15.0, 12.4 Hz, 1H), 1.69 (d, *J* = 18.8 Hz, 3H), 1.16 - 0.88 (m, 4H), 0.39 (tt, *J* = 19.4, 7.4 Hz, 6H); ¹³C NMR (100 MHz, D₂O) δ 175.19 (s), 168.99 (s), 147.42 (s), 142.18 (s), 131.94 (s), 130.72 (s), 128.57 (s), 124.51 (s), 124.06 (s), 84.16 (s),

74.95 (s), 53.05 (s), 52.66 (s), 49.05 (s), 38.68 (s), 28.39 (s), 25.38 (s), 25.03 (s), 24.49 (s), 22.31 (s), 8.46 (s), 8.42 (s). HRMS: m/z 514.2775 $[M+H]^+$, $C_{25}H_{35}N_7O_5$ (513.2700).

(3R,4R,5S)-4-acetamido-5-amino-N-(2-(1-(4-bromobenzyl)-1H-1,2,3-triazol-4-yl)ethyl)-3-(pentan-3-yloxy)cyclohex-1-ene-1-carboxamide (7b): Recrystallized from isopropyl ether as a white solid, yield 70 %, mp: 125-128 °C. 1H NMR (400 MHz, D_2O) δ 7.69 (s, 1H), 7.14 (d, $J = 8.0$ Hz, 2H), 6.91 (d, $J = 8.1$ Hz, 2H), 5.99 (s, 1H), 5.26 (s, 2H), 4.04 (d, $J = 8.2$ Hz, 1H), 3.94 - 3.63 (m, 1H), 3.42 (dd, $J = 16.6, 10.9$ Hz, 1H), 3.32 (s, 2H), 3.23 - 3.10 (m, 1H), 2.73 (s, 2H), 2.65 (d, $J = 13.1$ Hz, 1H), 2.47 - 2.21 (m, 1H), 1.90 (s, 3H), 1.35 - 1.06 (m, 4H), 0.55 (dt, $J = 24.1, 7.2$ Hz, 6H); ^{13}C NMR (100 MHz, D_2O) δ 175.00 (s), 168.68 (s), 133.72 (s), 132.25 (s), 131.84 (s), 130.57 (s), 129.90 (s), 122.20 (s), 83.67 (s), 74.92 (s), 53.45 (s), 52.67 (s), 49.09 (s), 38.64 (s), 28.48 (s), 25.51 (s), 25.13 (s), 24.45 (s), 22.45 (s), 8.77 (s), 8.56 (s). HRMS: m/z 547.2053 $[M+H]^+$, $C_{25}H_{35}BrN_6O_3$ (546.1954).

(3R,4R,5S)-4-acetamido-5-amino-N-(2-(1-(2-(hydroxymethyl)-5-(5-methyl-2,4-dioxo-3,4-dihydropyrimidin-1(2H)-yl)tetrahydrofuran-3-yl)-1H-1,2,3-triazol-4-yl)ethyl)-3-(pentan-3-yloxy)cyclohex-1-ene-1-carboxamide (7c): Recrystallized from isopropyl ether as a white solid, yield 57 %, mp: 202-205 °C. 1H NMR (400 MHz, D_2O) δ 7.88 (s, 1H), 7.63 (s, 1H), 6.30 (t, $J = 6.5$ Hz, 1H), 6.13 (s, 1H), 5.28 (dd, $J = 5.7, 2.7$ Hz, 1H), 4.30 (dd, $J = 8.9, 4.0$ Hz, 1H), 4.14 (d, $J = 8.7$ Hz, 1H), 3.91 (dd, $J =$

11.6, 9.0 Hz, 1H), 3.77 (dd, $J = 12.6, 3.1$ Hz, 1H), 3.66 (dd, $J = 12.6, 4.3$ Hz, 1H), 3.44 (ddd, $J = 18.9, 12.4, 6.4$ Hz, 3H), 3.35 (dd, $J = 11.0, 5.5$ Hz, 1H), 2.85 (t, $J = 6.3$ Hz, 2H), 2.78 (d, $J = 6.4$ Hz, 1H), 2.74 - 2.59 (m, 2H), 2.49 - 2.31 (m, 1H), 1.94 (s, 3H), 1.77 (s, 3H), 1.51 - 1.20 (m, 4H), 0.70 (dt, $J = 15.0, 7.4$ Hz, 6H); ^{13}C NMR (100 MHz, D_2O) δ 175.24 (s), 168.98 (s), 166.45 (s), 151.50 (s), 145.29 (s), 137.63 (s), 132.17 (s), 130.71 (s), 123.40 (s), 111.51 (s), 85.49 (s), 84.34 (d, $J = 6.0$ Hz), 75.08 (s), 60.60 (s), 59.73 (s), 52.68 (s), 49.15 (s), 38.89 (s), 36.99 (s), 28.41 (s), 25.48 (s), 25.11 (s), 24.58 (s), 22.37 (s), 11.54 (s), 8.53 (s). HRMS: m/z 603.3252 $[\text{M}+\text{H}]^+$, $\text{C}_{28}\text{H}_{42}\text{N}_8\text{O}_7$ (602.3176).

(3R,4R,5S)-4-acetamido-5-amino-N-(2-(1-(4-nitrobenzyl)-1H-1,2,3-triazol-4-yl)propan-2-yl)-3-(pentan-3-yloxy)cyclohex-1-ene-1-carboxamide (8a): Recrystallized from isopropyl ether as a white solid, yield 74 %, mp: 155-157 °C. ^1H NMR (400 MHz, D_2O) δ 8.18 (dd, $J = 42.6, 8.5$ Hz, 2H), 7.90 (s, 1H), 7.35 (d, $J = 8.7$ Hz, 2H), 6.26 (s, 1H), 5.64 (s, 2H), 4.20 (d, $J = 8.7$ Hz, 1H), 3.96 (dd, $J = 11.5, 9.0$ Hz, 1H), 3.62 - 3.33 (m, 2H), 2.69 (dt, $J = 25.6, 12.9$ Hz, 1H), 2.57 - 2.31 (m, 1H), 2.00 (s, 3H), 1.59 (s, 6H), 1.52 - 1.27 (m, 4H), 0.76 (dt, $J = 10.5, 7.4$ Hz, 6H); ^{13}C NMR (100 MHz, D_2O) δ 175.23 (s), 168.77 (s), 153.50 (s), 147.51 (s), 142.30 (s), 131.81 (s, $J = 41.9$ Hz), 131.40 (s), 128.60 (s), 124.13 (s), 122.74 (s), 84.35 (s), 75.07 (s), 53.35 - 53.12 (m), 52.82 (d, $J = 24.1$ Hz), 51.02 (s), 49.11 (s), 28.41 (s), 27.17 (s), 27.07 (s), 25.44 (s), 25.01 (s), 22.34 (s), 8.47 (s), 8.43 (s). HRMS: m/z 528.2930 $[\text{M}+\text{H}]^+$, $\text{C}_{26}\text{H}_{37}\text{N}_7\text{O}_5$ (527.2856).

(3R,4R,5S)-4-acetamido-5-amino-N-(2-(1-(4-bromobenzyl)-1H-1,2,3-triazol-4-yl)propan-2-yl)-3-(pentan-3-yloxy)cyclohex-1-ene-1-carboxamide (8b): Recrystallized from isopropyl ether as a white solid, yield 70 %, mp: 165-167 °C. ¹H NMR (400 MHz, D₂O) δ 7.54 (s, 1H), 7.14 (s, 2H), 6.83 (s, 2H), 5.96 (s, 1H), 5.15 (s, 2H), 3.91 (s, 1H), 3.67 (s, 1H), 3.14 (s, 2H), 2.40 (s, 1H), 2.13 (s, 1H), 1.71 (s, 3H), 1.22 (d, *J* = 44.6 Hz, 6H), 1.10 (d, *J* = 50.5 Hz, 4H), 0.47 (s, 6H); ¹³C NMR (100 MHz, DMSO) δ 171.00 (s), 166.42 (s), 153.57 (s), 136.12 (s), 132.11 (s), 131.87 (s), 131.56 (s), 130.63 (s), 122.01 (s), 121.78 (s), 81.49 (s), 74.62 (s), 53.02 (s), 52.36 (s), 51.16 (s), 49.63 (s), 29.12 (s), 28.59 (s), 28.55 (s), 26.15 (s), 25.48 (s), 23.82 (s), 9.86 (s), 9.46 (s). HRMS: *m/z* 561.2195[M+H]⁺, C₂₆H₃₇BrN₆O₃ (560.2111).

(3R,4R,5S)-4-acetamido-5-amino-N-(2-(1-(2-(hydroxymethyl)-5-(5-methyl-2,4-dioxo-3,4-dihydropyrimidin-1(2H)-yl)tetrahydrofuran-3-yl)-1H-1,2,3-triazol-4-yl)propan-2-yl)-3-(pentan-3-yloxy)cyclohex-1-ene-1-carboxamide (8c): Recrystallized from isopropyl ether as a white solid, yield 40%, mp: 180-183 °C. ¹H NMR (400 MHz, D₂O) δ 7.94 (s, 1H), 7.63 (s, 1H), 6.45 - 6.12 (m, 2H), 5.37 - 5.19 (m, 1H), 4.35 (s, 1H), 4.18 (d, *J* = 8.5 Hz, 1H), 4.03 - 3.81 (m, 1H), 3.79 (d, *J* = 12.3 Hz, 1H), 3.68 (dd, *J* = 12.5, 3.7 Hz, 1H), 3.44 (dd, *J* = 12.4, 5.6 Hz, 2H), 2.92 - 2.76 (m, 1H), 2.78 - 2.58 (m, 2H), 2.47 - 2.31 (m, 1H), 1.96 (s, 3H), 1.79 (s, 2H), 1.64 - 1.44 (m, 6H), 1.38 (ddd, *J* = 21.1, 13.5, 6.8 Hz, 4H), 0.88 - 0.56 (m, 6H); ¹³C NMR (100 MHz, DMSO) δ

171.02 (s), 166.44 (s), 164.21 (s), 153.54 (s), 150.93 (s), 136.75 (s), 131.90 (s), 131.54 (s), 121.53 (s), 110.09 (s), 85.03 (s), 84.36 (s), 81.49 (s), 74.61 (s), 61.23 (s), 59.55 (s), 53.02 (s), 51.17 (s), 49.64 (s), 37.51 (s), 29.14 (s), 28.66 (s), 28.50 (s), 26.15 (s), 25.46 (s), 23.81 (s), 12.71 (s), 9.86 (s), 9.45 (s). HRMS: m/z 617.3402 $[M+H]^+$, $C_{29}H_{44}N_8O_7$ (616.3333). HPLC purity: 94.43%.

4.2. *In vitro* NA Inhibitory Assay

The NA inhibition assay was carried out according to the standard method [20-22, 26]. Influenza virus A/Goose/Guangdong/SH7/2013 (H5N1), A/Chicken/Hebei/LZF/2014 (H5N2) and A/Duck/Guangdong/674/2014 (H5N6) were kindly provided by Institute of Poultry Science, Shandong Academy of Agricultural Sciences. The H5N1-H274Y NA was obtained from Sino Biological Inc. The substrate used in the enzyme inhibition assay, MUNANA (M8639) which could be cleaved by NA to yield a quantifiable fluorescent product, was purchased from Sigma. Influenza virus suspensions were obtained from the allantoic fluid of the chicken embryo layer. The tested compounds were dissolved and diluted to the corresponding concentrations in MES buffer (32.5 mM 2-(N-morpholino)ethanesulfonic acid, 4 mM $CaCl_2$, pH 6.5). In a 96-well plate, 10 μ L of the diluted virus supernatant, 70 μ L of MES buffer, and 10 μ L of compounds at different concentrations were added successively and incubated at 37 °C for 10 min. Then the reaction was started by the addition of the 10 μ L of substrate. After incubation for 40 min, 150 μ L of 0.2 M glycine-NaOH (pH = 10.2) were added in the solution to terminate the reaction solution. Fluorescence was recorded (excitation at 365 nm and emission at 460 nm), and substrate blanks were

subtracted from the sample readings. The 50% inhibitory concentration (IC_{50}) was calculated by plotting the percent inhibition of NA activity versus the inhibitor concentration.

4.3. Molecular docking

Molecular simulations of molecule **61** was performed using the Tripos molecular modeling package Sybyl-X 2.0. Compound **61** was optimized using the Tripos force field for 1000-generations until the maximum derivative of energy became 0.005 kcal/(mol*Å). Charges were computed and added according to Gasteiger-Huckel parameters. The flexible docking method (Surflex-Dock) docked the ligand automatically into the ligand-binding site of the receptor by the use of protocol-based approach and an empirically derived scoring function. The published three dimensional crystal structures of NA complexes (PDB: 2HU0 and 5HUM)) were retrieved from the Protein Data Bank, and the proteins were prepared by removing the ligand, water molecules, and other unnecessary small molecules; then polar hydrogen atoms and charges were added to the protein. After the protomol was generated, the optimized molecule was surflex-docked into the binding pocket of NAs, with the relevant parameters set as defaults. Top-scoring pose was shown by the software of PyMOL version 1.5 (www.pymol.org) [26, 27].

4.4. *In vitro* anti-influenza virus assay and cytotoxicity assay in chicken embryo fibroblast (CEFs)

The anti-influenza activity (EC_{50}) and cytotoxicity (CC_{50}) of the newly synthesized oseltamivir derivatives were evaluated with H5N1, H5N2 and H5N6 strains in

Chicken Embryo Fibroblasts (CEFs) using Cell Counting Kit-8 (CCK-8, Dojindo Laboratories) method as described by Zhang et al [21, 27-28]. EC_{50} are the concentrations of compound required for 50% protection of the influenza virus infection-mediated cytopathic effects (CPE). The tested compounds and positive control were dissolved in DMSO and serially diluted by 3-fold in media (1 % FBS in DMEM). Mixture of 100 μ L diluted influenza virus (100 $TCID_{50}$) and equal volumes of solutions of the test compounds at different concentrations was added to the cells and incubated at 37 °C under 5% CO_2 . After incubation for 48 h, 100 μ L Cell Counting Kit-8 reagent solution (10 μ L CCK-8 in 90 μ L media) was added according to the manufacturer's manual. After incubating at 37°C for 90 min, the absorbance at 450 nm was read on a microplate reader. The EC_{50} values were determined by fitting the curve of percent cytopathic effect (CPE) versus inhibitor concentration. The CC_{50} values (50% cytotoxic concentrations) of newly synthesized inhibitors to CEFs were determined by the procedure similar to the EC_{50} but without virus infection.

4.5 *In vivo* anti-influenza activity in Specific Pathogen Free (SPF) chicken embryonated egg.

Specific Pathogen Free (SPF) chicken embryonated eggs were incubated horizontally at 37 °C and a relative humidity of 50 % for 9-11 days and then were candled to eliminate infertile eggs and dead embryos. A 1 mm diameter hole was drilled into the egg shell on the side where the embryo was located, and avoided accidental damage of the underlying shell membrane. Then the mixtures of 0.2 ml virus (200 $TCID_{50}$)

and equal volume of different concentrations of tested compounds were incubated for 1 h, and injected into the eggs from the hole. Next, the hole was sealed by wax and the eggs were incubated horizontally under standard conditions described above. After 72 h, the viability of the chick embryos was checked by candling the eggs. At the same time, to study the effect of the operational procedure on the viability of the chick embryos, eggs were handled as the same as the treatment experiments, but only treated with 0.9 % NaCl (no virus and compounds), and as control experiments, the eggs were inoculated by the mixture of virus and 0.9 % NaCl. Finally, the number of the survival and death were recorded to evaluate the anti-influenza activity of the compounds [22, 26, 30].

Conflict of interest

The authors declare no conflict of interest.

Acknowledgments

Financial support from the National Natural Science Foundation of China (NSFC no. 81773574), Shandong Provincial Key Research and Development Program (no. 2017CXGC1401, 2015GNC110009), Major agricultural applied technological innovation Project of Shandong Province (no. SD2019XM006), the Science and Technology Development Project of Shandong Province (no. 2014GSF118175), Major Project of Science and Technology of Shandong Province (no. 2015ZDJS04001), Agricultural scientific and technological innovation project of

Shandong Academy of Agricultural Sciences (no. CXGC2016B14).

References and notes

- [1] [https://www.who.int/en/news-room/fact-sheets/detail/influenza-\(seasonal\)](https://www.who.int/en/news-room/fact-sheets/detail/influenza-(seasonal)).
- [2] H.V. Fineberg, Pandemic preparedness and response-lessons from the H1N1 influenza of 2009, *N Engl J Med.* 370 (2014) 1335-42.
- [3] S. Mohan, P.S. Kerry, N. Bance, M. Niikura, B.M. Pinto, Serendipitous discovery of a potent influenza virus A neuraminidase inhibitor, *Angew. Chem. Int. Edit.* 53 (2014) 1076-1080.
- [4] C. Xu, L. Dong, L. Xin, Y. Lan, Y. Chen, L. Yang, Y. Shu, Human avianinfluenza A (H5N1) virus infection in China, *Sci. China Ser. C Life Sci.* 52 (2009) 407-411.
- [5] S. Zheng, L. Tang, H. Gao, Y. Wang, F. Yu, D. Cui, G. Xie, X. Yang, W. Zhang, X. Ye, Z. Zhang, X. Wang, L. Yu, Y. Zhang, S. Yang, W. Liang, Y. Chen, L. Li, Benefit of early initiation of neuraminidase inhibitor treatment to hospitalized patients with avian influenza A(H7N9) virus, *Clin. Infect. Dis.* 66 (2018) 1054-1060.
- [6] K. Subbarao, T. Joseph, Scientific barriers to developing vaccines against avian influenza viruses, *Nat. Rev. Immunol.* 7 (2007) 267-278.
- [7] J. Gong, W. Xu, J. Zhang, Structure and functions of influenza virus neuraminidase, *Curr Med Chem.* 14 (2007) 113-122.
- [8] N. Lee, A.C. Hurt, Neuraminidase inhibitor resistance in influenza: a clinical perspective, *Curr Opin Infect Dis.* 31 (2018) 520-526.
- [9] M. Samson, A. Pizzorno, Y. Abed, G. Boivin, Influenza virus resistance to

- neuraminidase inhibitors, *Antiviral Res.* 98 (2013) 174-185.
- [10] P.J. Collins, L.F. Haire, Y.P. Lin, J.F. Liu, R.J. Russell, P.A. Walker, J.J. Skehel, S.R. Martin, A.J. Hay, S.J. Gamblin, Crystal structures of oseltamivir-resistant influenza virus neuraminidase mutants, *Nature.* 453 (2008) 1258-1261.
- [11] R. Trebbien, S.S. Pedersen, K. Vorborg, K.T. Franck, T.K. Fischer, Development of oseltamivir and zanamivir resistance in influenza A(H1N1)pdm09 virus, *Euro Surveill.* 22 (2017) pii: 30445.
- [12] C.Y. Tai, P.A. Escarpe, R.W. Sidwell, M.A. Williams, W. Lew, H. Wu, C.U. Kim, D.B. Mendel, Characterization of human influenza virus variants selected in vitro in the presence of the neuraminidase inhibitor GS 4071, *Antimicrobial Agents & Chemotherapy.* 42 (1998) 3234-3241.
- [13] S.S. Kode, S.D. Pawar, D.S. Tare, S.S. Keng, A.C. Hurt, J. Mullick, A novel I177T substitution in neuraminidase of highly pathogenic avian influenza H5N1 virus conferring reduced susceptibility to oseltamivir and zanamivir, *Vet Microbiol.* 235 (2019) 21-24.
- [14] R.J. Russell, L.F. Haire, D.J. Stevens, P.J. Collins, Y.P. Lin, G.M. Blackburn, A.J. Hay, S.J. Gamblin, J.J. Skehel, The structure of H5N1 avian influenza neuraminidase suggests new opportunities for drug design, *Nature.* 443 (2006) 45-49.
- [15] R.E. Amaro, D.D.L. Minh, L.S. Cheng, W.M. Lindstrom, A.J. Olson, J.H. Lin, W.W. Li, J.A. McCammon, Remarkable loop flexibility in avian influenza N1 and its implications for antiviral drug design, *J Am Chem Soc.* 129 (2007) 7764-7765.
- [16] R.E. Amaro, X. Cheng, I. Ivanov, D. Xu, J.A. McCammon, Characterizing loop

dynamics and ligand recognition in human- and avian-type influenza neuraminidases via generalized born molecular dynamics and end-point free energy calculations, *J Am Chem Soc.* 131 (2009) 4702-4709.

[17] E. Feng, W.J. Shin, X. Zhu, J. Li, D Ye, J. Wang, M. Zheng, J.P. Zuo, K.T. No, X. Liu, W. Zhu, W. Tang, B.L. Seong, H. Jiang, H. Liu, Structure-based design and synthesis of C-1- and C-4-modified analogs of zanamivir as neuraminidase inhibitors. *J Med Chem.*56 (2013) 671-84.

[18] B. Wang, K. Wang, P. Meng, Y. Hu, F. Yang, K. Liu, Z. Lei, B. Chen, Y. Tian, Design, synthesis, and evaluation of carboxyl-modified oseltamivir derivatives with improved lipophilicity as neuraminidase inhibitors, *Bioorg Med Chem Lett*, 28 (2018) 3477-3482.

[19] P.H. Hsu, D.C. Chiu, K.L. Wu, P.S. Lee, J.T. Jan, Y.E. Cheng, K.C. Tsai, T.J. Cheng, J.M. Fang, Acylguanidine derivatives of zanamivir and oseltamivir: Potential orally available prodrugs against influenza viruses, *Eur J Med Chem*, 154 (2018) 314-323.

[20] Y. Xie, D. Xu, B. Huang, X. Ma, W. Qi, F. Shi, X. Liu, Y. Zhang, W. Xu, Discovery of N-substituted oseltamivir derivatives as potent and selective inhibitors of H5N1 influenza neuraminidase, *J. Med. Chem.*, 57 (2014) 8445-8458.

[21] J. Zhang, V. Poongavanam, D. Kang, C. Bertagnin, H. Lu, X. Kong, H. Ju, X. Lu, P. Gao, Y. Tian, H. Jia, S. Desta, X. Ding, L. Sun, Z. Fang, B. Huang, X. Liang, R. Jia, X. Ma, W. Xu, N.A. Murugan, A. Loregian, B. Huang, P. Zhan, X. Liu, Optimization of N-substituted oseltamivir derivatives as potent inhibitors of group-1 and -2

influenza A neuraminidases, including a drug-resistant variant, *J. Med. Chem.* 61 (2018) 6379-6397.

[22] J. Zhang, N.A. Murugan, Y. Tian, C. Bertagnin, Z. Fang, D. Kang, X. Kong, H. Jia, Z. Sun, R. Jia, P. Gao, V. Poongavanam, A. Loregian, W. Xu, X. Ma, X. Ding, B. Huang, P. Zhan, X. Liu, Structure-based optimization of N-substituted oseltamivir derivatives as potent anti-influenza A virus agents with significantly improved potency against oseltamivir-resistant N1-H274Y variant, *J. Med. Chem.* 61 (2018) 9976-9999.

[23] S. Cavalli, A.R. Tipton, M. Overhand, A. Kros, The chemical modification of liposome surfaces via a copper-mediated [3+2] azide-alkyne cycloaddition monitored by a colorimetric assay, *Chem. Commun.* 30 (2006) 3193-3195.

[24] H.F. Said, B. Frisch, F. Schuber, Targeted liposomes: convenient coupling of ligands to preformed vesicles using "click chemistry", *Bioconjugate Chem.* 17 (2006) 849-854.

[25] X. Wang, B. Huang, X. Liu, P. Zhan, Discovery of bioactive molecules from CuAAC click-chemistry-based combinatorial libraries, *Drug Discov Today.* 21 (2016) 118-132.

[26] H. Ju, J. Zhang, Z. Sun, Z. Huang, W. Qi, B. Huang, P. Zhan, X. Liu, Discovery of C-1 modified oseltamivir derivatives as potent influenza neuraminidase inhibitors, *Eur J Med Chem.* 146 (2018) 220-231.

[27] R. Jia, J. Zhang, W. Ai, X. Ding, S. Desta, L. Sun, Z. Sun, X. Ma, Z. Li, D. Wang, B. Huang, P. Zhan, X. Liu, Design, synthesis and biological evaluation of

"Multi-Site"-binding influenza virus neuraminidase inhibitors, *Eur J Med Chem.* 178 (2019) 64-80.

[28] J.J. Shie, J.M. Fang, S.Y. Wang, K.C. Tsai, Y.S. Cheng, A.S. Yang, S.C. Hsiao, C.Y. Su, C.H. Wong, Synthesis of Tamiflu and its phosphonate congeners possessing potent anti-influenza activity, *J. Am. Chem. Soc.* 129 (2007) 11892-11893.

[29] D.E. Clark, S.D. Pickett, Computational methods for the prediction of 'drug-likeness', *Drug Discovery Today.* 5 (2000) 49-58.

[30] A. Sauerbrei, A. Haertl, A. Brandstaedt, M. Schmidtke, P. Wutzler, Utilization of the embryonated egg for in vivo evaluation of the anti-influenza virus activity of neuraminidase inhibitors, *Med Microbiol Immunol.* 195 (2006) 65-71.

Highlights

- By exploiting the 430-cavity of influenza virus neuraminidase, a series of 1,2,3-triazole oseltamivir derivatives were reported.
- Compound **6l** possessed the most potent and broad-spectrum anti-influenza activity in both enzymatic assay and cellular assay.
- Molecular docking studies showed that **6l** adopted the similar binding modes with Group-1 and Group-2 neuraminidases.
- Compound **6l** achieved the similar protective effect against H9N2 strain with OSC in the embryonated egg model.

Declaration of interests

The authors declare that they have no known competing financial interests or personal relationships that could have appeared to influence the work reported in this paper.

The authors declare the following financial interests/personal relationships which may be considered as potential competing interests: